POLYETHYLENIMINE-CAPPED GOLD NANOPARTICLES IN NUCLEIC ACID DELIVERY

by

Aykut Hınık

BSc. in Molecular Biology and Genetics, Boğaziçi University, 2019

Submitted to the Institute of Biomedical Engineering
in partial fulfillment of the requirements
for the degree of
Master of Science
in
Biomedical Engineering

Boğaziçi University
2023

ACKNOWLEDGMENTS

First of all, I would like to express my most sincere gratitude to Assoc. Prof. Dr. Ömer Aydın for his guidance, hospitality, and the opportunities he provided in the laboratory during my studies. I am thankful to Prof. Dr. Cengizhan Öztürk for his support and guiding. I would like to thank to Dr. Cansu Ümran Tunç for sharing her valuable wet lab experience with me. I am also thankful to the thesis committee members Prof. Dr. Gökhan Demirel, Asst. Prof. Dr. Necla Birgül İyison, and Asst. Prof. Dr. Banu İyisan for their time and attention.

Here, I would like to share my gladness for working with Dilek Kanarya, Furkan Esen, Furkan Özben, Gizem Kurşunluoğlu, Münevver Akdeniz, Nada Walveel, Orhan Ekşi, Şerife Güvendi, Ümmügülsüm Yılmaz, and Zakarya Al-Shaebi in NanoTheraLab. I would like to recall my precious friends Ali Yurtseven, Azad Fırat Genç, Betül Efe, Bilal Başdağ, Ebrar Karakaya, Ecem Gülnihal, Enes Okatar, Elif Özlem Topal, Fatih Soğukpınar, Fevzi Yüksel, Dr. Mert Can Çavuş, and Sezgin Mengi for being my supporter all the time.

Last but not least, I would like to emphasize the endless thrust and support of my dear family Yeşim & Ömer Ay, Dr. Yeliz & Dr. Kenan Özendi, Hülya & Yetiş Hınık, and Derin & Metehan.

This thesis was funded by Turkish Scientific and Technological Research Council (TUBITAK) (Project No: 120S938).

In the memory of my dear friend Dt. Ahmet Hüsrev Çelik.

February 2023

ACADEMIC ETHICS AND INTEGRITY STATEMENT

I, Aykut Hınık, hereby certify that I am aware of the Academic Ethics and Integrity Policy issued by the Council of Higher Education (YÖK) and I fully acknowledge all the consequences due to its violation by plagiarism or any other way.

Name :

Signature:

Date:

ABSTRACT

POLYETHYLENIMINE-CAPPED GOLD NANOPARTICLES IN NUCLEIC ACID DELIVERY

RNA interference is a gene editing tool applicable in cancer therapy. Nucleic acid delivery into the cells is challenging due to nucleic acid instability, insufficient cellular uptake, and endosomal entrapment. Polyethylenimine (PEI) is a positively charged polymer molecule widely used in nucleic acid delivery. PEI ensures increased endosomal escape thanks to the proton sponge effect. However, PEI is known to be highly toxic because of molecular size and electrical charge. Gold nanoparticles (AuNPs) are attractive inorganic carriers with biocompatibility, easy synthesis, and adaptability of surface chemistry. In this study, it was aimed to synthesize polyethylenimine-capped gold nanoparticles (AuPEI-NPs) to investigate their cytotoxicity and nucleic acid delivery in breast cancer cells compared to free PEI. Resazurin assay demonstrated that AuPEI-NPs induced less cytotoxicity than free PEI until the 20 µg/ml concentration in breast cancer cells. Flow cytometry demonstrated that AuPEI-NPs yielded significantly higher cellular uptake of fluorescently tagged siRNA than PEI. In conclusion, this study demonstrated that AuPEI-NPs are promising nucleic acid carriers in gene therapy with a less cytotoxicity and better cellular uptake than free PEI in breast cancer cells.

Keywords: Gene Therapy, Gold Nanoparticle (AuNP), Nucleic Acid Delivery, Polyethylenimine (PEI), Small Interfering RNA (siRNA)

ÖZET

NÜKLEİK ASİT İLETİMİNDE POLİETİLENİMİN KAPLI ALTIN NANOPARÇACIKLAR

RNA interferansı, kanser tedavisinde uygulanabilen bir gen düzenleme aracıdır. Nükleik asit kararsızlığı, yetersiz hücresel alım ve endozomal tuzak nedeniyle hücrelere nükleik asit iletimi zordur. Polietilenimin (PEI), nükleik asit iletiminde yaygın olarak kullanılan pozitif yüklü bir polimer molekülüdür. PEI, proton sünger etkisi nedeniyle artmış endozomal kaçış sağlar. Bununla birlikte, PEI'nin moleküler boyutu ve elektrik yükü nedeniyle oldukça toksik olduğu bilinmektedir. Altın nanoparçacıklar (AuNP'ler), biyouyumluluk, kolay sentez ve yüzey kimyasının uyarlanabilirliği nedeniyle cazip inorganik taşıyıcılardır. Bu çalışmada, polietilenimin kaplı altın nanoparçacıkların (AuPEI-NP'ler) sentezi ve meme kanseri hücrelerinde sitotoksisite ve nükleik asit iletiminin serbest PEI'ye kıyasla araştırılması amaçlandı. Resazurin tahlili, AuPEI-NP'lerin meme kanseri hücrelerinde 20 µg/ml konsantrasyona kadar serbest PEI'den daha az sitotoksisiteye sebep olduğunu gösterdi. Flow sitometri, AuPEI-NP'lerin PEI'ye göre önemli ölçüde daha yüksek floresan etiketli siRNA'nın hücresel alımını sağladığını gösterdi. Sonuç olarak, bu çalışma, AuPEI-NP'lerin, meme kanseri hücrelerinde serbest PEI'den daha az sitotoksisite ve daha iyi hücresel alım ile gen terapisinde umut verici nükleik asit taşıyıcıları olduğunu göstermiştir.

Anahtar Sözcükler: Gen Terapi, Altın Nanoparçacık (AuNP), Nükleik Asit İletimi, Polietilenimin (PEI), Küçük İnterferans RNA'sı (siRNA)

TABLE OF CONTENTS

LIST OF FIGURES

LIST OF TABLES

LIST OF SYMBOLS

°C	Celcius
Cu^{2+}	Copper (II) ion
kDa	Kilodalton
μg	Microgram
μL	Microliter
mg	Milligram
mV	Millivolt
%	Percentage
nm	Nanometer
N/P	Amine to Phosphate Ratio

LIST OF ABBREVIATIONS

Bcl-2	B-Cell Leukemia/Lymphoma 2
DOX	Doxorubicin
$HAuCl_4$	Hydrogen Tetrachloroaurate
AuNP	Gold Nanoparticle
AuPEI-NP	Polyethylenimine-Capped Gold Nanoparticle
DLS	Dynamic Light Scattering
FAM	Carboxyfluorescein
IC	Inhibitory Concentrations
$Na_3C_6H_5O_7$	Trisodium Citrate
PDI	Polydispersity Index
PEI	Polyethylenimine
RNAi	RNA Interference
siRNA	Small Interfering RNA

1. INTRODUCTION

Breast cancer is the most widespread cancer type around the world. World Health Organization (WHO) reported that more than 2.3 million people were diagnosed with and 685,000 died from breast cancer in 2020. WHO also predicted 3 million diagnoses and 1 million deaths per year by 2040 based on the world demographic trends [1].

One major cause of most cancers is the failure in the control of programmed cell death, also called apoptosis. Apoptosis is the genetically controlled process in which damaged and uninvited cells are eliminated for the sake of physiological function and development of multicellular organisms [2]. In the case of defects in the regulation of apoptosis, the uninvited cells could survive and reproduce uncontrollably, causing the emergence of pathological conditions, including degenerative diseases and cancers.

B-Cell Leukemia/Lymphoma 2 (Bcl-2) is a critical gene in apoptotic regulation. Bcl-2 protein takes a role in mitochondrial outer membrane permeability to cytochrome c and other apoptotic factors, which can start a cascade of events leading to apoptosis once localised in cytosol [3].

Chemotherapy is a conventional approach in cancer treatment, in which toxic drugs are utilized to terminate cancer cells. Anthracyclines are the most common chemotherapy drugs, two of which are doxorubicin (DOX) and daunorubicin (DNR). DOX intercalates into DNA helices and covalently binds to the proteins functioning in the replication of DNA and translation processes, eventually leading to cell death [4].

Although chemotherapy drugs are highly toxic, following the continuous mono-chemotherapy application that targets a single modality of the cancer, cancer cells can accumulate mutations that provide them with resistance to multiple chemotherapeutic agents with some similarity as a result of replicative immortality. This situation is

known as multidrug resistance (MDR), resulted in the emergence of the need for new therapeutic approaches including combination therapy and gene therapy [5].

Combination therapy is a fashionable approach in cancer therapy, consisting of the simultaneous application of an anti-cancer strategy with chemotherapy for a better therapeutic outcome. Combination therapy aims to provide with a synergistic effect in which the combined treatment achieves an actual therapeutic impact even greater in comparison to the expected additive effect of each separate therapeutic approaches [6]. As a result of combination therapy, drug sensitivity of cancer cells can be increased, which makes possible a chemotherapy plan at a lower drug dose to decrease side effects and toxicity. In combination therapy, a chemotherapy drug can be combined with another chemotherapy drug, as well as with gene therapy or phototherapy [5].

Gene therapy is a bioengineering strategy of inducing modifications of a gene sequence or gene expression profile related to a pathological phenotype. This can be applied by gene editing, gene addition or gene silencing. In guidance of a nucleic acid sequence complementary to a specific gene, precise genetic manipulation can be provided. Genome of an organism can be edited based on endonucleatic cleavage and repair of the DNA by ZFNs, TALENs, and CRISPR/Cas9. On the other hand, gene expression can be manipulated by RNA interference (RNAi) at the post-transcriptional level while keeping the genome intact [7].

RNA interference (RNAi) is a mechanism of recognition and manipulation of RNA transcripts by use of short RNAs in 20 to 30 nucleotide length. RNAi is a natural defense mechanism against the invasion of viruses and transposable elements in many eukaryotes [8]. Through Watson–Crick base pairing with the mRNA molecules, RNAi agents can silence mRNA transcripts by mRNA degradation or translation inhibition [9]. MicroRNAs and small interfering RNAs are among the RNAi agents.

MicroRNAs (miRNAs) are regulatory RNAs, taking role in post-transcriptional gene silencing. In order to inhibit translation, miRNA binds to a mRNA transcript at the $3'$ untranslated region, reducing its interaction with the translation machinery [10].

miRNAs can also induce mRNA degradation incorporated with RNA-induced silencing complex (RISC) within Argonaute pathway [11].

Small interfering RNAs (siRNAs) are double-stranded in 20-25 nucleotide length. In order to get functional, siRNA molecules are processed by a specific RNAse called Dicer in the cytoplasm. Then, the siRNA molecule gets attached with RNA-induced silencing complex (RISC), where it is processed into a single-stranded RNA. The processed siRNA guides the RISC complex to identify the mRNA targets to be degraded by Argonaute 2 [12] (Figure 1.1).

Bcl-2 is an oncogene overexpressed in breast cancer cells. In cancer gene therapy, Bcl-2 has been selected as a major target [13], as it is associated with drug resistance in cancer therapy [14]. Bcl-2 small interfering RNA (Bcl-2 siRNA) has been utilized for inhibiting Bcl-2 expression at the mRNA level [15].

Although RNAi is promising in cancer treatment based on silencing of oncogenes like Bcl-2, there are some difficulties to be considered. RNAi agents required to be successfully delivered into target cell cytoplasm to be functional [16]. On the other hand, delivery of the RNAi agents into the cells might be challenging [17] (Figure 1.2).

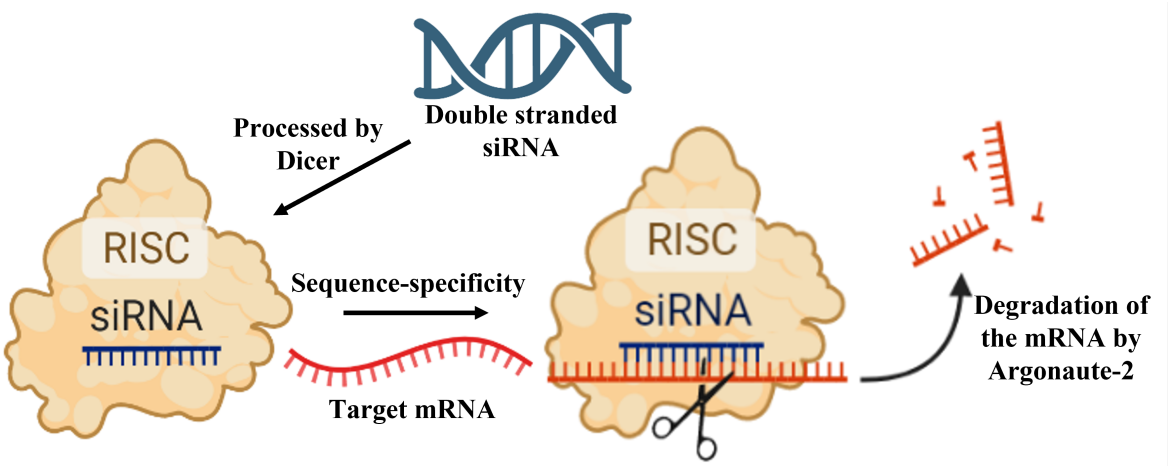

Figure 1.1 Molecular mechanism of siRNA-mediated gene silencing. The figure was produced by using BioRender templates.

.

First of all, free nucleic acids are not long-lasting as they can be easily degraded by nucleases. Following the delivery of nucleic acids into blood circulation, nuclease and phosphatase enzymes in the body induce quick degradation of nucleic acids into fragments within phosphodiester bonds before the intact therapeutic agents can arrive and accumulate in the intended region [17].

In addition, the cellular uptake of free nucleic acids is not sufficient for an effective gene therapy because the negatively charged cellular membrane is not permeable to nucleic acids [18]. Although cellular uptake of nucleic acids can take place through endocytic pathways [16], the nucleic acids are often entrapped inside the endosomes and eventually degraded within endolysosomal pathway [19].

Achieving a successful therapeutic result in RNAi is one of the goals of gene delivery research. Nucleic acid delivery can utilize viral vectors and physical non-viral gene delivery systems. Nucleic acid delivery strategies also include chemical modifications of the nucleic acids and the development of delivery systems utilizing differ-

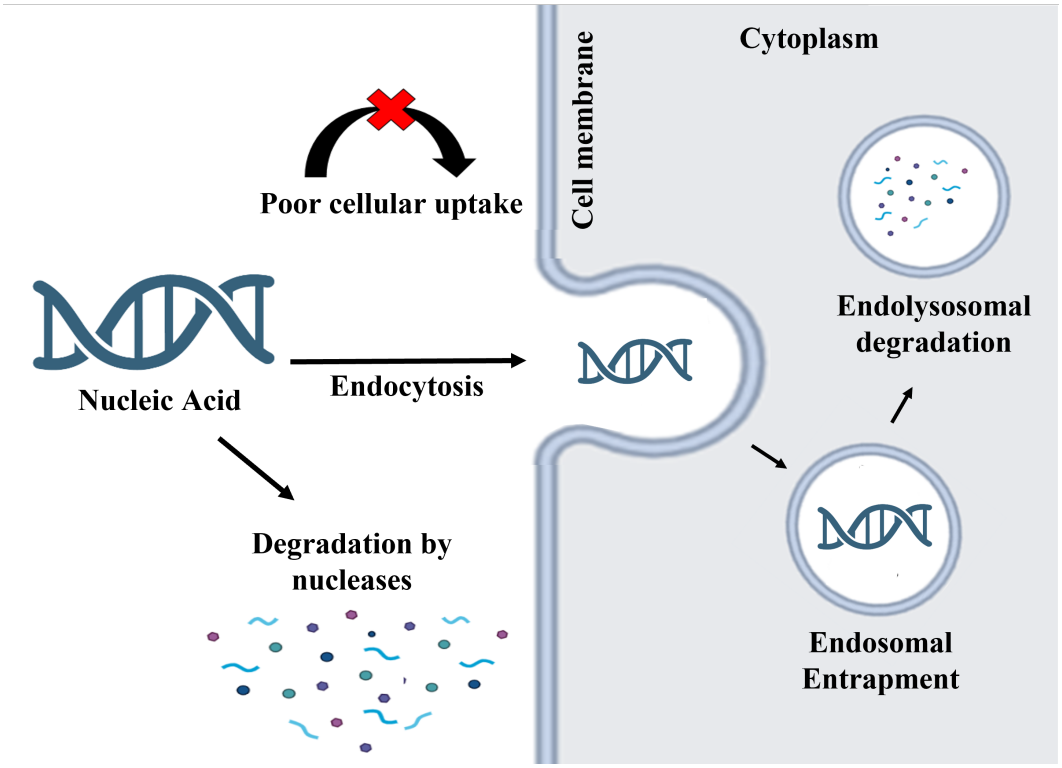

Figure 1.2 Challenges in nucleic acid delivery. The figure was produced by using BioRender templates.

ent materials such as lipids, lipidoids, peptides, exosomes, polymers, and inorganic nanoparticles [17].

Viral vector systems are widely used in nucleic acid delivery. Recombinant viruses include lentiviruses, retroviruses, adenoviruses, and AAVs. Although viral vectors are quite efficient in gene delivery due to the enhanced cellular uptake by intracellular trafficking, they might trigger relatively higher immunogenic and oncogenic effects [20].

Physical non-viral delivery systems include jet injection, hydrodynamic gene transfer, gene gun, and electroporation [20]. Physical non-viral delivery is relatively easier to prepare than viral vectors, producing lower immune reaction, and available for the delivery of genes of larger size [21].

Jet injection is a physical non-viral gene delivery strategy, which is applied to the organism using pressurized gas at high-speed. On the other hand, jet injection might cause local pain, edema, and bleeding. Hydrodynamic gene transfer simply uses increased liquid pressure by producing pores on cell membranes for increased permeability. On the other hand, the need for high doses and non-specificity restrict its clinical use [20].

Gene gun is a gene delivery method in which unmodified genetic agents or nanoparticles conjugated with genetic material are injected into cells. Electroporation produces temporary pores on cell membranes by the applied electrical field for the gene delivery, but its *in vivo* use is highly restricted [20].

For the purpose of nucleic acid delivery, nanoparticle delivery systems have been developed. One advantage of nanoparticles in nucleic acid delivery is that physicochemical properties of a nanoparticle can be engineered to modulate cytotoxicity, membrane permeability, and the kinetics of the nucleic acid uptake into the cell [20].

To achieve a successful nucleic acid delivery, the nanoparticles should be biocom-

patible, non-immunogenic, and biodegradable while providing efficient cellular uptake. Once conjugated to a nanoparticle, the nucleic acids can be protected from serum inactivation and enzymatic degradation. Nanoparticle conjugation can also enhance cellular uptake and avoid endosomal entrapment. [12].

In the blood circulation, nanoparticles are prone to accumulate at the inflammation and tumor sites that are under the increased need of nutrient and oxygen supply. As a result of impaired lymphatic function at the tumor site, relatively large sized nanoparticles with low diffusibility start accumulating selectively at the tumor sites, a phenomenon named enhanced permeability and retention (EPR) effect. This allowes for the biomedical agents to be targeted to tumor sites for therapeutic and imaging purposes [22].

The nanoparticle structures utilized in gene delivery include inorganic, polymeric, and solid lipid nanoparticles, liposomes, nanocrystals, nanotubes, and dendrimers [20].

One contemporary example for nanoparticle-based nucleic acid delivery systems is the SARS-CoV-2 vaccines. mRNA-1273 (Moderna) and BNT162b2 (Pfizer-BioNTech) are the examples for SARS-CoV-2 vaccines constituted by lipid nanoparticles (LNP). This nanoparticle systems aims to deliver mRNAs to the cytoplasm to produce viral antigens in SARS-CoV-2 immunity [23].

Cationic polymers are commonly utilized in nucleic acid delivery. They complex with anionic nucleic acids to form polyplexes in nano size, often more stable than lipoplexes, containing cationic lipids. The cytotoxicity is affected by the size, molecular weight, and the polymer/DNA charge ratios of the polyplexes [20].

Polyethylenimine (PEI) is a positively charged polymer molecule, built by the repetition of one amine group and two aliphatic carbons (ethylenimine) in a linear or branched array (Figure 1.3). Linear PEI contains only primary and secondary amines, while branched PEI might contain primary, secondary and tertiary amines. Linear PEI

is found in solid phase at the room temperature with a melting point around 74 °C and it is soluble in organic solvents and hot water under acidic conditions. On the other hand, branched PEI is dense and viscous at RT [24].

Concentration of polyethylenimine cannot be measured with UV-vis spectroscopy because PEI does not contain a chromophore group. On the other hand, when PEI interacts with copper (II) ions (Cu^{2+}), formation of a dark blue cuprammonium complex is observed, which can be characterised with absorption peaks at 285 nm and 630

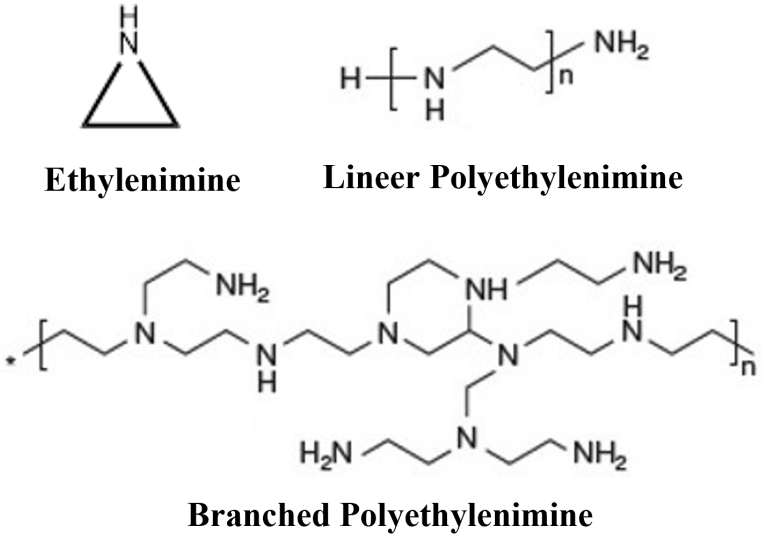

Figure 1.3 Chemical structure of ethylenimine and polyethylenimine (PEI) in linear and branched forms

.

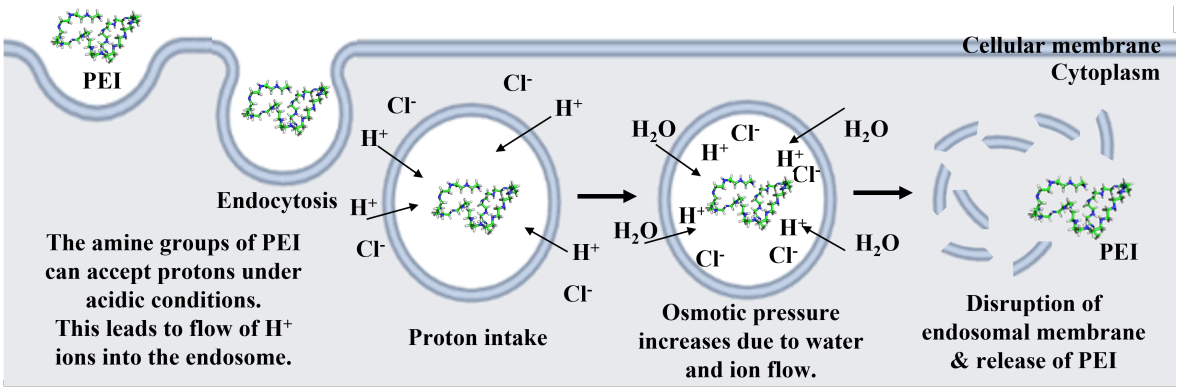

Figure 1.4 Endosomal escape of polyethylenimine due to proton sponge effect. The figure was produced by using BioRender templates.

nm. Absorbance of cuprammonium complex is linearly related to PEI concentration in a solution. In the presence of copper (II) sulfate, the concentration of PEI is estimated based on the absorbance at 285 nm in reference to the absorbance of PEI with known concentration [25].

Under acidic conditions, branched PEI acts as a proton acceptor because of its secondary and tertiary amines. This provides PEI with a buffering capacity in solution, described by the hypothesis of proton sponge effect (Figure 1.4) [26]. According to this hypothesis, once inside an endosome, PEI starts gathering protons, resulting in a flow of protons from the cytoplasm to the endosome. Proton intake leads to the accumulation of counter ions resulting in enhanced osmotic pressure in the endosome. High osmotic pressure makes the endosomal membrane disrupt so that PEI is released to the cytosol (Figure 1.4). Beside endosome escape, PEI might also increase the stability of a cargo inside an endolysosome by stabilizing the low pH of endolysosomal pH, resulting in the inactivation of degradative enzymes [27].

PEI has been widely used in nucleic acid delivery based on electrostatic interactions [24]. On the other hand, PEI is highly toxic because of its positive electrical charges that might cause disruption of cellular membrane integrity, leading to necrosis [28].

Cytotoxicity of PEI also depends on its molecular size as huge PEI clusters could aggregate outside surface of the cell membrane, which triggers necrosis [29]. Nonetheless, small molecular weight PEI was reported to be nontoxic but at the same time ineffective in nucleic acid delivery [30].

Reduction of molecular size of PEI by forming a compact nanoparticle structure could be a strategy to reduce cytotoxicity while preserving nucleic acid delivery success [31]. In the presence of PEI, reduction of metals into compact colloids can be achieved for the purpose of nucleic acid delivery [32].

Inorganic nanoparticles are hydrophilic, highly stable, and biocompatible ma-

terials with low cytotoxicity. Gold, silver, and iron oxide nanoparticles are among the inorganic nanoparticles extensively utilized in biomedical applications including nucleic acid delivery [33]. Gold nanoparticles (AuNPs) are attractive inorganic carriers in nucleic acid delivery considering their biocompatibility, relatively less cytotoxicity, easy synthesis, and adaptability of surface chemistry [34] [35].

Gold nanoparticles in various geometries have been formulated and utilized in biomedical applications, including gold nanospheres, nanorods, nanostars, and nanocones. The size and geometry of AuNPs have an impact on the delivery and biodistribution of the cargo as well as their biological utilization and therapeutic efficiency [36]. The size, geometry, and surface functionalization of AuNPs can be relatively easily established. As a result of this, the nanoparticle formulations can be adjusted according to the biological purpose [37].

Gold nanoparticles have some characteristic optical properties useful in their detection. Surface plasmon resonance (SPR) is a phenomenon which occurs within nanoparticle form of noble metals as a result of confinement of photons into a small nanoparticle size [38]. Mie Theory suggested that gold nanoparticles have unique light scattering profiles according to their sizes allowing for size estimation based on the absorbance at the surface plasmon resonance [39].

Negatively charged spherical gold nanoparticles between 10-30 nm sizes can be synthesized by reducing hydrogen tetrachloroaurate ($HAuCl_4$) with trisodium citrate ($Na_3C_6H_5O_7$) in high temperature, known as the Turkevich method [40]. For nucleic acid delivery purpose, negatively charged gold nanoparticles can be conjugated with thiol functionalized nucleic acids with salt aging method [41].

Synthesis of positively charged gold nanoparticles can be established by using amine-functionalized molecules as reductants and stabilizers [42]. According to a model, tertiary amines of PEI act as both reductant and stabilizer during the synthesis of polyethylenimine-capped gold nanoparticles (AuPEI-NPs). The tertiary amine groups get tightly bound to colloidal gold thanks to the lone electron pairs. After

gold-amine complexes are formed, thermal decomposition occurs very rapidly, during which amine molecules prevent gold nanoparticles from further aggregation [43].

Polyethylenimine capped gold nanoparticles (AuPEI-NPs) have been utilized in biomedical applications including Surface-Enhanced Raman Scattering (SERS) [42], glutathione sensing [32], and nucleic acid delivery [44] (Figure 1.5).

AuPEI-NPs has been utilized in the delivery of green fluorescent protein (GFP) siRNA to silence the GFP protein expression in MDA-MB-435 human breast carcinoma [44]. Delivery of GFP siRNA by AuPEI-NPs achieved GFP silencing with AuPEI-NPs more successfully than free PEI, although cellular uptake with AuPEI-NPs was not as high as with free PEI. Enhanced apoptosis was also achieved in MDA-MB-435 when the expression of polo-like kinase 1 (PLK1) was silenced with PLK1 siRNAs carried by AuPEI-NPs [44].

In another study, targeted delivery of AuPEI-NPs to prostate cancer cells has been achieved. Following the synthesis, AuPEI-NPs were conjugated with folic acid (FA) to target prostate-specific membrane antigen (PSMA), a folate receptor overexpressed in LNCaP human prostate adenocarcinoma cells. It was reported that cellular uptake of AuPEI-NP/FA conjugates into LNCaP cells was more successful than PC-3

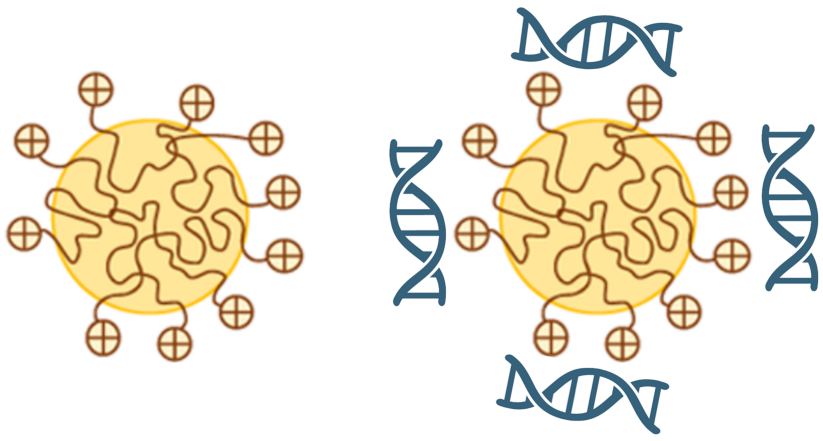

Figure 1.5 Demonstration of the structure of polyethylenimine-capped gold nanoparticles with siRNA. In the demonstration, the sizes of AuPEI-NPs and siRNA are accepted as 13 nm and 7.5 nm, respectively.

.

prostate cancer cells without folate receptor expression, concluding targeted delivery of AuPEI-NPs/FA conjugates in prostate cancer [45].

In this study, it was aimed to synthesize polyethylenimine-capped gold nanoparticles (AuPEI-NPs) to investigate their cytotoxicity and nucleic acid delivery in MDA-MB-231 breast cancer cell line to compare with free PEI. It was also aimed to investigate the use of AuPEI-NPs in gene therapy as a carrier for the delivery of siRNAs to breast cancer cells to silence oncogenic Bcl-2 protein expression in order to reduce cancer cell growth and colony formation.

2. MATERIALS AND METHODS

In this study, polyethylenimine-capped gold nanoparticles (AuPEI-NPs) were synthesized by reducing hydrogen tetrachloroaurate ($HAuCl_4$) with branched 25 kDa polyethylenimine at 60 °C. The nanoparticle characterisation was conducted with UV-vis spectroscopy and dynamic light scattering (DLS). Optimal amine to phosphate ratio was determined with agarose gel retardation assay. Cell viability experiments were conducted with resazurin (alamar blue) assay. Efficiency of cell delivery was determined with flow cytometry and fluorescence microscopy. Gene expression levels were determined with western blot. Crystal violet staining was applied for a colony formation assay.

2.1 Materials

Hydrogen tetrachloroaurate ($HAuCl_4$), 25 kDa branched polyethylenimine, distilled water, Perkin Elmer Lambda 35 UV-vis Spectrophotometer, Malvern Nano ZetaSizer (ZS), Promega Glomax Multi Detection System, UV transilluminator, Flow Cytometer, Fluorescence Microscope, Semi-dry transfer device, capillary zeta cells, quartz micro cuvettes, DMEM, FBS, Penicillin, Trypsin, Bcl-2 siRNA, GAPDH siRNA, Fluorescein amidite (FAM)-tagged siRNA, Doxorubicin, crystal violet, paraformaldehyde, resazurin reagent, agarose, ethidium bromide, RIPA buffer, Coomassie reagent, bovine serum albumin, Laemmli Buffer, Protein Ladder, TBS-T, running buffer, transfer buffer, whatman papers, PVDF membrane, milk powder, Bcl-2 antibody, GAPDH antibody, IgG secondary anti rabbit antibody, ECL reagent, shaker, centrifuge

2.2 Synthesis and Preparation of the Nanoparticles

Polyethylenimine-capped gold nanoparticles (AuPEI-NPs) were prepared by reducing hydrogen tetrachloroaurate ($HAuCl_4$) in the presence of 25 kDa branched polyethylenimine. During the reaction, polyethylenimine behaved as a reductant and stabilizer [32]. The synthesis was conducted at room temperature, 60 °C, and 65 °C to determine optimal synthesis protocol.

In the synthesis at 60 °C and 65 °C, 544 µl of $HAuCl_4$ 10 % was added into 22 ml warm distilled water. 6 ml of 25 kDa branched PEI 1 % was added. The reaction took place at 60 °C or 65 °C for 15 min [32]. Densities were 1.94 mg/ml $HAuCl_4$ and 2.14 mg/ml PEI in 28.5 ml final volume (Figure 2.1).

In the synthesis at room temperature, 119 µl of $HAuCl_4$ 10 % was added into 25 ml distilled water. 500 µl of 25 kDa branched PEI 1 % was adjected. The solution was agitated at 720 rpm at ambient temperature for 24 hours [44]. Densities were 0,466 mg/ml $HAuCl_4$ and 0,196 mg/ml PEI in 25,6 ml final volume.

To purify AuPEI-NPs from the residual PEI, centrifugation at 15000 rpm was applied for 20 min the next day after synthesis. The supernatant was removed com-

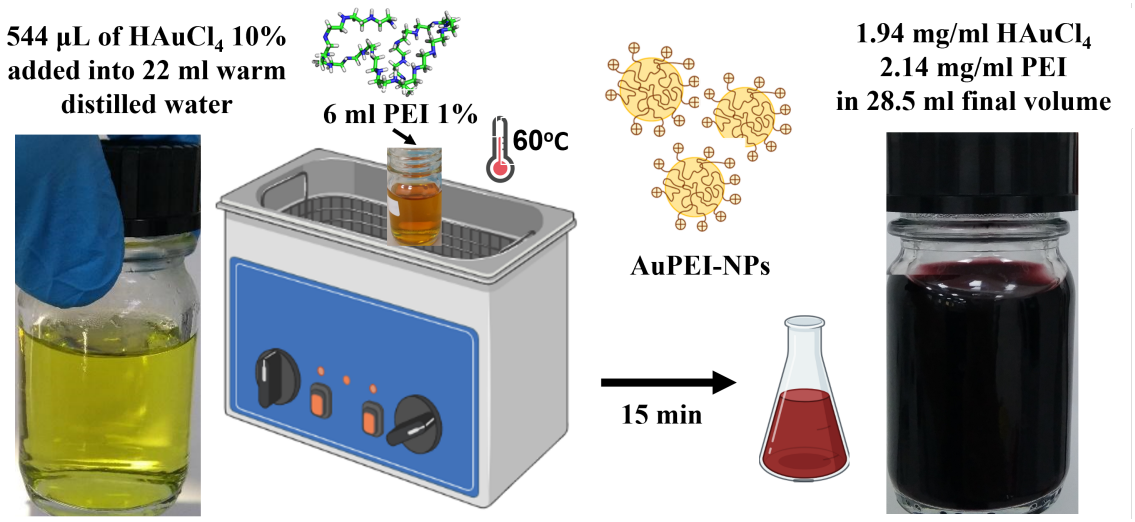

Figure 2.1 Synthesis of AuPEI-NPs at 60 °C for 15 min. The figure was produced by using BioRender templates.

pletely and the pellet was dissolved with distilled water in the same volume with the supernatant. After 2 days the centrifugation step was repeated.

To determine a protocol for PEI quantification to measure amount of PEI in AuPEI-NPs after purification by centrifugation, coomassie blue staining was applied to PEI with known concentrations and the supernatant of the AuPEI-NPs centrifugation. For this purpose, PEI was prepared in 2, 4, 8, and 16 µg/ml concentrations. 10 μl of PEI was added to 200 μl coomassie reagent. Absorbance at 595 nm is measured with plate reader and a standard curve for PEI was drawn (Figure A.1). In comparison to the PEI standard curve, PEI concentration in the supernatant after centrifugation was calculated to determine how much PEI was contained in AuPEI-NPs.

In the thesis, the synthesis and characterisation of gold nanospheres and nanocones were also included to demonstrate different gold nanoparticle formulations (Figure 2.2). The synthesis of negatively charged gold nanoparticles were conducted by citrate reduction based on the Turkevich method [46]. Gold nanocones were synthesized based

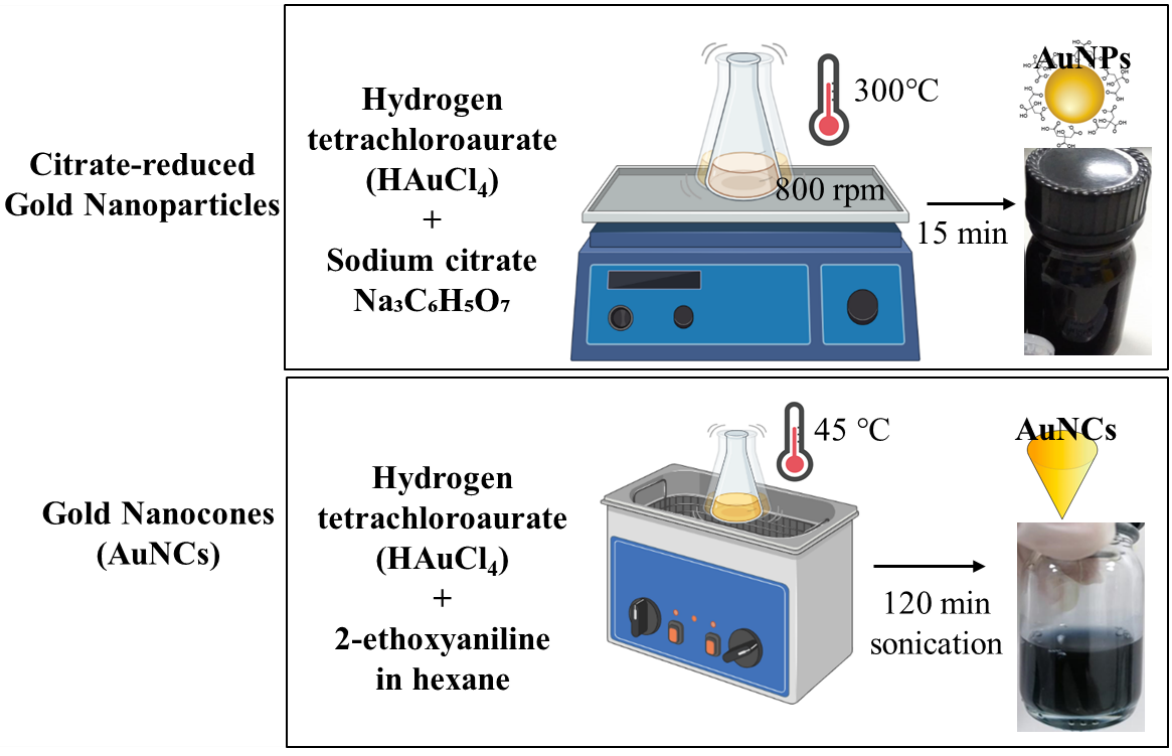

Figure 2.2 Synthesis of citrate-reduced gold nanoparticles and gold nanocones. The figure was produced by using BioRender templates.

on reduction of gold in the presence of 2-ethoxyaniline in hexane with ultrasonic application at 45 °C for 120 minutes [47].

2.3 Nanoparticle Characterisation

2.3.1 UV-vis Spectroscopy

The characterisation was performed with Perkin Elmer Lambda 35 UV-vis Spectrophotometer and Quant Lambda 25 software between 400 nm and 800 nm wavelengths. Prior to the measurement, 1/10 dilution of the AuPEI-NPs sample was prepared. 2 ml of sample was placed in a quartz micro cuvette. Distilled water was used as a blank. Wavelength versus absorbance was plotted with Graph Pad Prism 8.

2.3.2 Dynamic Light Scattering (DLS)

Z-average size and zeta potential were measured with Malvern Nano ZetaSizer. Prior to the measurement, 1/10 dilution of the AuPEI-NPs sample was prepared. Following the injection of 750 µl of sample into the capillary zeta cell, zeta potential measurement was performed. 2 ml of sample was placed in quartz micro cuvette for size measurements. During the measurement, solvent and material parameters were selected as distilled water and gold, respectively. Diagrams of size versus intensity percent and zeta potential versus intensity count were plotted with Graph Pad Prism 8.

2.4 Cytotoxicity of Free PEI and AuPEI-NPs

Cytotoxicity of free PEI and AuPEI-NPs in breast cancer cells was analyzed with resazurin (alamar blue) assay, based on metabolic reduction of resazurin in viable cells (Figure 2.3). MDA-MB-231 cells were nurtured in full medium (DMEM with 10

% FBS and 1 % penicillin) at 37 °C under 5 % CO_2. The cells were regularly passaged after arriving at 70-80 % confluency.

In the experiment, 10,000 cells in 200 µl medium per well were seeded and they were allowed for 24 hours for attachment to the plate surface. During the treatment, the medium was repleted with PEI or AuPEI-NPs in relevant concentrations in DMEM. The media containing free PEI and AuPEI-NPs were prepared with a serial dilution method in 10, 20, 40, 80, and 160 µg/ml PEI concentrations. 5 repeats were applied for each control and experimental group. Following the treatment, they were left at 37 °C under 5 % CO_2 for 2 days.

To determine the cell viability, resazurin reagent was applied to the cells. The media were changed with 200 µl of 1 X resazurin solution, which was prepared by diluting 20 X resazurin reagent in fresh media. The cells were incubated in 1 X resazurin at 37 °C under 5 % CO_2 for 3 hours. Cellular viability was detected by measuring fluorescence at 595 nm with Promega Glomax Multi Detection System. The fluorescence values were normalized due to empty wells. Cell viability percentage of each experimental group was calculated in reference to the untreated group by accepting the untreated group 100 % viable. PEI concentration versus cell viability percent was plotted with Graph Pad Prism 8. Statistical significance between free PEI and AuPEI-NPs was determined by t-test for each PEI concentration.

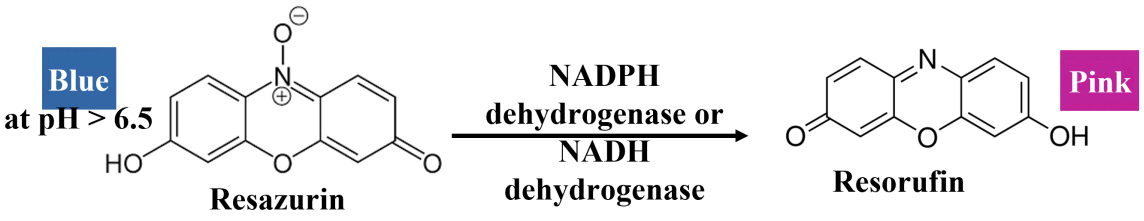

Figure 2.3 Resazurin is metabolized into resorufin in viable cells. Resazurin is a nontoxic and cell-permeable metabolite which is weakly fluorescent, while resorufin is the highly fluorescent metabolic product of resazurin. The metabolisation of resazurin to resorufin is an indicator of aerobic respiration of viable cells [48].

Table 2.1 PEI and siRNA amounts (nmol) for different amine to phosphate ratios (N/P)

N/P	**0**	**1/2**	**1/1**	**2/1**	**4/1**	**5/1**
siRNA	0.04	0.04	0.04	0.04	0.04	0.04
Phosphate	1.68	1.68	1.68	1.68	1.68	1.68
PEI	0	0.00145	0.0029	0.0058	0.0116	0.0145
Amine	0	0.84	1.68	3.36	6.72	8.4

2.5 Determining Optimum Ratio of AuPEI-NPs and siRNA

Optimum ratio of AuPEI-NPs and siRNA was determined by agarose gel retardation assay. AuPEI-NPs were complexed with siRNA at room temperature based on electrostatic interactions. AuPEI/siRNA complexes were prepared using 1 µl of siRNA in various amine to phosphate (N/P) ratios (Table 2.1). AuPEI/siRNA complexes were loaded onto 2 % agarose gel with 5 % ethidium bromide and mobilized at 120 V for 35 minutes. Electrophoretic motility of siRNA was visualized under UV to determine the optimal N/P ratio in which complete siRNA loading to AuPEI-NPs takes place.

2.6 Cellular Uptake of siRNAs Carried by Free PEI and AuPEI-NPs to Breast Cancer Cells

2.6.1 Flow Cytometry

Flow cytometry was applied to measure the efficiency of the delivery of fluorescein amidite (FAM)-tagged siRNA to breast cancer cells through PEI or AuPEI-NPs.

In the experiment, 60,000 cells were incubated in 500 µl full medium for 1 day for attachment to the plate surface at 37 °C under 5 % CO_2. PEI/siRNA and AuPEI/siRNA were complexed at room temperature in an N/P of 4/1 in 250 µl of FBS-free DMEM. 4 hours following the treatment, the cells were supplemented with

250 µl DMEM with 20 % FBS. Final siRNA concentration was equal to 50 nM for each experimental group. 3 repeats were applied for each control and experimental group.

Cellular uptake was measured with flow cytometry for green fluorescence, 2, 4, 6, and 20 hours after the treatment. Time versus cellular uptake percentage was plotted Graph Pad Prism 8. Statistical significance between free PEI and AuPEI-NPs was determined by t-test for each time point.

2.6.2 Fluorescence Microscopy

Internalization of fluorescein amidite (FAM)-tagged siRNA was determined via fluorescence microscopy. In the experiment, 100,000 cells in 2 ml full media per well were seeded directly onto glass slides placed in the wells of a plate and left at 37 °C under 5 % CO_2 for 1 day.

Before treatment, PEI/siRNA and AuPEI/siRNA were complexed at room temperature in an N/P of 4/1 in 1000 µl of FBS-free DMEM. 4 hours following the treatment, the cells were supplemented with 1000 µl DMEM with 20 % FBS. Final siRNA concentration was equal to 50 nM for each group. The cells on the glass slides were fixed in paraformaldehyde 4 % 4 hrs, 6 hrs, and 24 hrs following the therapy and stored at 4 °C. The internalization of FAM-tagged siRNA was investigated through a fluorescence microscope for excitation wavelength 495 nm.

2.7 Protein Expression Following Bcl-2 siRNA Delivery by Free PEI and AuPEI-NPs

Bcl-2 was targeted with Bcl-2 siRNAs carried by free PEI and AuPEI-NPs in breast cancer cells. In the experiment, 300,000 cells in 2 ml full medium were allowed for 1 day for attachment to the plate surface at 37 °C under 5 % CO_2.

Before the treatment, PEI/siRNA and AuPEI/siRNA were complexed at room temperature in an N/P of 4/1 in 1 ml of FBS-free DMEM. 4 hours after the treatment, they were supplemented with 1 ml DMEM with 20 % FBS. Final siRNA concentrations were 50 nM and 100 nM for both free PEI and AuPEI-NPs experimental groups. Following the treatment, they were left at 37 °C under 5 % CO_2 for 2 days. The cells were collected into a tube after detached from plate surface by trypsin treatment.

2.7.1 Western Blot

It was applied to demonstrate silencing of Bcl-2 protein expression in breast cancer cells, after the application of Bcl-2 siRNAs carried by free PEI and AuPEI-NPs. Protein was extracted from the cell pellet with RIPA buffer and vortexing. Protein concentration of the cellular extracts were determined by measuring absorbance at 595 nm following coomassie blue staining in reference to the bovine serum albumin (BSA) protein standard curve.

Polyacrylamide gel was prepared as 4 % stacking gel and 10 % separation gel. Total protein in 75 µg amount was analyzed in SDS-PAGE (80 V, 15 min + 100 V, 120 min). The protein bands were transferred onto a PVDF membrane at 20 V for 15 min with semi-dry transfer. The membrane blocking was performed with 5 % milk powder for 120 minutes. Then, it was treated with anti-rabbit Bcl-2 antibody at 4 °C for 18 hours, 3 washes with PBS-T were applied. Then it was treated with IgG rabbit antibody, 3 washes with PBS-T and 1 wash with PBS were applied. Following treatment with ECL reagent, the Bcl-2 protein bands were visualized with UV transilluminator and BIO-RAD ImageLab 6.1 Software. After detecting Bcl-2 protein level, the membrane was treated with anti-rabbit GAPDH antibody and the same protocol was applied to visualize GAPDH protein bands.

2.8 Therapeutic Effect of Free PEI and AuPEI-NPs Mediated Gene Therapy on Breast Cancer Cells

2.8.1 Growth Inhibition Assay

Resazurin assay was applied to determine growth inhibition of breast cancer cells, following the application of Bcl-2 siRNA carried by PEI or AuPEI-NPs. In the experiment, 2000 cells in 0.2 ml medium/well were seeded and grown for 1 day. Before the treatment, PEI/siRNA and AuPEI/siRNA were complexed at room temperature in an N/P of 4/1 in 100 µl of FBS-free DMEM for each well. 4 hours following the treatment, the cells were supplemented with 100 µl DMEM with 20 % FBS, completing final volume of each well to 200 µl. Final siRNA concentrations were 50 nM and 100 nM for both free PEI and AuPEI-NPs experimental groups, with final PEI concentrations 0,37 mg/ml and 0,75 mg/L, respectively. 5 repeats were applied for each control and experimental group and incubated at 37 °C under 5 % CO_2 for 72 hours. Then, resazurin assay was applied to determine cellular viabilities.

2.8.2 Colony Formation Assay

The assay was applied by crystal violet staining to determine the reduction in colony formation of breast cancer cells by the treatment with Bcl-2 siRNA carried by PEI or AuPEI-NPs. In the experiment, 1000 cells in 250 µl medium/well were seeded and grown for 1 day. Before the treatment, PEI/siRNA and AuPEI/siRNA were complexed at room temperature in an N/P of 4/1 in 100 µl of FBS-free DMEM for each well.

4 hours following the treatment, the cells were supplemented with 250 µl DMEM with 20 % FBS, completing final volume of each well to 500 µl. Final siRNA concentrations were 50 nM and 100 nM for both free PEI and AuPEI-NPs experimental groups, with final PEI concentrations 0.36 mg/ml and 0.72 mg/L, respectively. 3 repeats were applied for each control and experimental group. Following the treatment, the cells

were left at 37 °C under 5 % CO_2 for 8 days. After removing the medium, the colonies were dyed with crystal violet to determine the number of the colonies.

3. RESULTS

3.1 Nanoparticle Synthesis

Reducing hydrogen tetrachloroaurate ($HAuCl_4$) solution in the presence of 25 kDa branched polyethylenimine at 60 °C and at 65 °C resulted in formation of wine red colored polyethylenimine-capped gold nanoparticles (AuPEI-NPs) in 15 minutes (Figure 3.1). On the other hand, synthesis at room temperature for 24 hours with continuous stirring ended up with a solution in pinkish red because of less $HAuCl_4$ concentration in the reaction (Figure 3.1).

3.2 Characterisation of the Nanoparticles

AuPEI-NPs were analyzed with UV-vis spectroscopy and DLS. UV-vis spectroscopy measured a maximum optical density at 520 nm for the AuPEI-NPs synthesized at 60 °C. Dynamic light scattering analysis showed + 37 mV zeta potential and 55 nm Z-average size with an PDI of 0.210. Zeta potential distribution plot confirmed the most counted zeta potential value to be 37 mV. Size distribution plot demonstrated the intensity of 13 nm sized nanoparticles as 22 % (Figure 3.2).

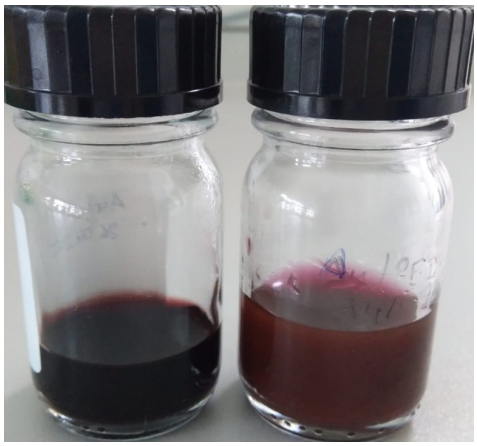

Figure 3.1 Appearance of AuPEI-NPs synthesized at 60 °C (left) and room temperature (right)

UV-vis spectroscopy characterized the AuPEI-NPs synthesized at room temperature and 65 °C with peaks at 530 nm and 520 nm, respectively. DLS measured Z-average sizes of AuPEI-NPs synthesized at room temperature and 65 °C as 36 nm and 207 nm, respectively. DLS characterized zeta potentials of AuPEI-NPs synthesized at both room temperature and 65 °C as 45 mV (Figure 3.2).

Free polyethylenimine (PEI) was also characterized with UV-vis spectroscopy and DLS (Figure 3.2). The optical density of free PEI was smaller than 0.025 between 400 nm and 1000 nm wavelength range (Figure 3.2). Z-average size of free PEI was measured as 145 nm and zeta potential of PEI was measured around +4 mV (Figure

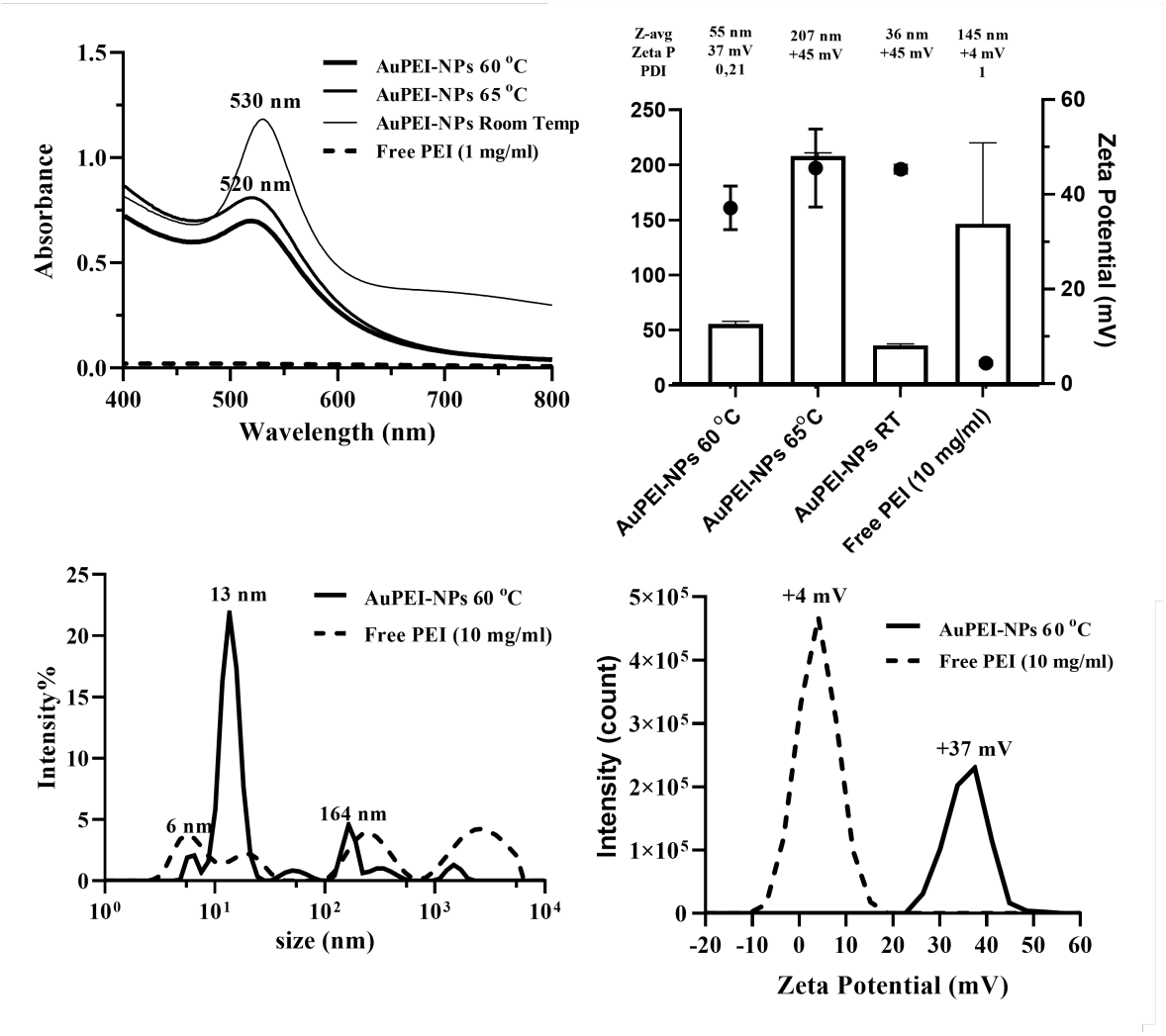

Figure 3.2 Characterisation of AuPEI-NPs and free PEI. (upper left) Ultraviolet–visible spectroscopy and (upper right) DLS analysis of AuPEI-NPs and free PEI. (lower left) Zeta potential and (lower right) size distribution of AuPEI-NPs and free PEI. Figures were drawn with Graphpad Prism 9 Software.

3.2).

The nanoparticles were characterised after purified with centrifugation by Ultraviolet–visible spectroscopy and DLS. AuPEI-NPs synthesised at 60 °C were characterized with absorbance peaks at 520 nm, 524 nm, and 533 nm before centrifugation, after the 1st centrifugation and after the 2nd centrifugation, consecutively (Figure 3.3).

Z-average sizes of AuPEI-NPs synthesised at 60 °C were determined 53 nm, 83 nm, and 109 nm before centrifugation, after the 1st centrifugation and after the 2ns centrifugation, consecutively (Figure 3.3). Zeta potential values of AuPEI-NPs synthesized at 60 °C were determined 37 mV, 46 mV, and 30 mV before centrifugation, after the 1st centrifugation and after the 2ns centrifugation, consecutively (Figure 3.3).

Z-average sizes of AuPEI-NPs synthesised at room temperature were determined 54 nm, 91 nm, and 126 nm before centrifugation, after the 1st centrifugation and after the 2ns centrifugation, consecutively. Zeta potential values of AuPEI-NPs synthesised at room temperature were determined 54 mV, 49 mV, and 24 mV before centrifugation, after the 1st centrifugation and after the 2ns centrifugation, consecutively (Figure 3.3).

To determine a PEI quantification protocol, PEI was stained with coomassie blue and absorbance was measured. A linear relationship between PEI concentration and absorbance at 595 nm was obtained with an R-square of 0,97 for 2, 4, 8, and 16 µg/ml the PEI concentrations (Figure A.1). The PEI in AuPEI-NPs synthesized at 60 °C was estimated 69.3 % and 64.5 % of the PEI amount added during synthesis after first and second centrifugation steps, respectively (Table A.1). On the other hand, the PEI in AuPEI-NPs synthesized at room temperature was estimated 22 % of the PEI amount added during synthesis after the both centrifugation steps (Table A.1).

Citrate-reduced spherical gold nanoparticles were characterized with an optical density peak at 526 nm by UV-vis spectroscopy, confirming gold nanoparticle formation. Dynamic light scattering measured 16 nm Z-average and -25 mV zeta potential for citrate-reduced gold nanoparticles (Figure 3.4). Gold nanocones were characterised

with a trough point around 500 nm wavelength in UV-vis spectroscopy. Dynamic light scattering measured Z-average of the gold nanocones as 350 nm. For gold nanocones, zeta potential was determined as +44 mV by dynamic light scattering, characterising it as a highly positively charged nanoparticle (Figure 3.4).

3.3 Cytotoxicity of AuPEI-NPs and Free PEI

Following synthesis and characterization of AuPEI-NPs, their cytotoxicity was measured. Cellular viability of breast cancer cells were measured by resazurin assay after free PEI and AuPEI-NPs treatment. Resazurin assay demonstrated no cytotoxicity for 2.5 µg/ml of AuPEI-NPs with 100 % cell viability, while 2.5 µg/ml of free PEI demonstrated 88 % cell viability. 5 µg/ml of AuPEI-NPs demonstrated 79 % cell viability. Cellular viability was obtained significantly higher for AuPEI-NPs than PEI for 2.5, 5, 10, and 20 µg/ml based on t-test with $p < 0.005$ (Figure 3.5).

3.4 Determination of the Optimum Ratio of AuPEI-NPs to siRNA

The optimum Ratio of AuPEI-NPs to siRNA was determined with agarose gel retardation assay for N/P ratios of 1/2, 1/1, 2/1, 4/1, 5/1, 10/1, 15/1, 20/1, 25/1, and 40/1. The assay demonstrated no electromotility of siRNAs for 4/1 and higher N/P ratios, concluding optimal siRNA loading in 4/1 N/P ratio (Figure 3.6).

3.5 Cellular Uptake of siRNAs Carried by Free PEI and AuPEI-NPs to Breast Cancer Cells

The internalization of FAM-tagged siRNAs to breast cancer cells was studied with flow cytometry and fluorescence miscoscopy.

3.5.1 Flow Cytometry

The delivery of FAM-tagged siRNA by free PEI and AuPEI-NPs to breast cancer cells was tracked by flow cytometry. 2 hours following the treatment, no cellular uptake was observed for both free PEI and AuPEI-NPs. 4 hours following the treatment, Student's t-test suggested significantly higher cellular uptake for AuPEI-NPs with 5 % compared to PEI with 3 % with $p < 0.05$. 6 hours following the therapy, cellular uptake of free PEI and AuPEI-NPs became insignificant, as it was 6 % for both. 20 hours after the treatment cellular uptake of AuPEI increased to 10 %, while that of PEI reduced to 3 %, suggesting a statistical difference with $p < 0.005$ by t-test (Figure 3.7).

3.5.2 Fluorescence Microscopy

The internalization of FAM-tagged siRNAs into breast cancer cells was determined with fluorescence microscopy. Cellular internalization was higher with AuPEI-NPs than PEI after 4th, 6th and 24th hours of the treatment. Cellular uptake was determined better with AuPEI-NPs at 4th hours and 24th hours after the treatment. Cellular uptake with PEI was not clear until the 24th hour of the treatment (Figure 3.8).

3.6 Protein Expression Following Bcl-2 siRNA Delivery by Free PEI and AuPEI-NPs

3.6.1 Western Blot

The total protein concentration of cellular extracts were determined by coomassie blue staining as in Table B.1 based on bovine serum albumin standard curve (Figure B.1) and total protein in 75 µg amount was analyzed in SDS-PAGE to determine Bcl-2

protein level of breast cancer cells. Bcl-2 protein level was not reduced by 50 nM Bcl-2 siRNA carried by AuPEI-NPs and PEI (Figure 3.9).

3.7 Therapeutic Effect of Free PEI and AuPEI-NPs Mediated Gene Therapy on Breast Cancer Cells

3.7.1 Growth Inhibition Assay

Cellular growth of breast cancer cells exposed to Bcl-2 siRNAs and GAPDH siRNAs carried by AuPEI-NPs and free PEI combined with doxorubicin IC 20 was measured by resazurin assay to determine growth inhibition of cancer cells (Figure 3.10). Untreated group was indicated with 100 % viability. Treatment with doxorubicin IC 20 resulted in 91.7 % viability. It was observed that in all the experimental groups, PEI treatment resulted in less cellular viability than AuPEI-NPs. Treatment with 100 nM Bcl-2 siRNA carried by free PEI reduced cellular viability to 90.9 %, suggesting significantly more growth inhibition than AuPEI-NPs delivery.

Combined therapy of doxorubicin IC 20 and 100 nM Bcl-2 siRNA carried by free PEI reduced cellular viability to 87.7 %. The treatment with 50 nM of GAPDH siRNA carried by both AuPEI-NPs and free PEI and 100 nM of siRNAs by AuPEI-NPs reduced cell viability to 94 %, suggesting statistically more growth inhibition than their Bcl-2 counterparts. The treatment with 100 nM GAPDH siRNA carried by PEI reduced cellular viability to 92.2 %, suggesting a significantly more growth inhibition than AuPEI-NPs delivery. Combined therapy of DOX IC 20 and GAPDH siRNA carried by free PEI reduced cellular viability to 87.6 % for 50 nM and 88.3 % for 100 nM siRNA concentrations (Figure 3.10).

3.7.2 Colony Formation Assay

The assay was applied with crystal violet to investigate the impact of Bcl-2 siRNA carried by free PEI and AuPEI-NPs on breast cancer cells (Figure 3.11). Untreated breast cancer cells formed denser colonies than the treatment groups. Delivery of Bcl-2 siRNA in 50 nM concentration by both AuPEI-NPs and free PEI resulted in less colony formation than the other experimental groups. The number of colonies was similar for 100 nM siRNA delivery and only nanoparticle groups for both AuPEI-NPs and free PEI (Figure 3.11).

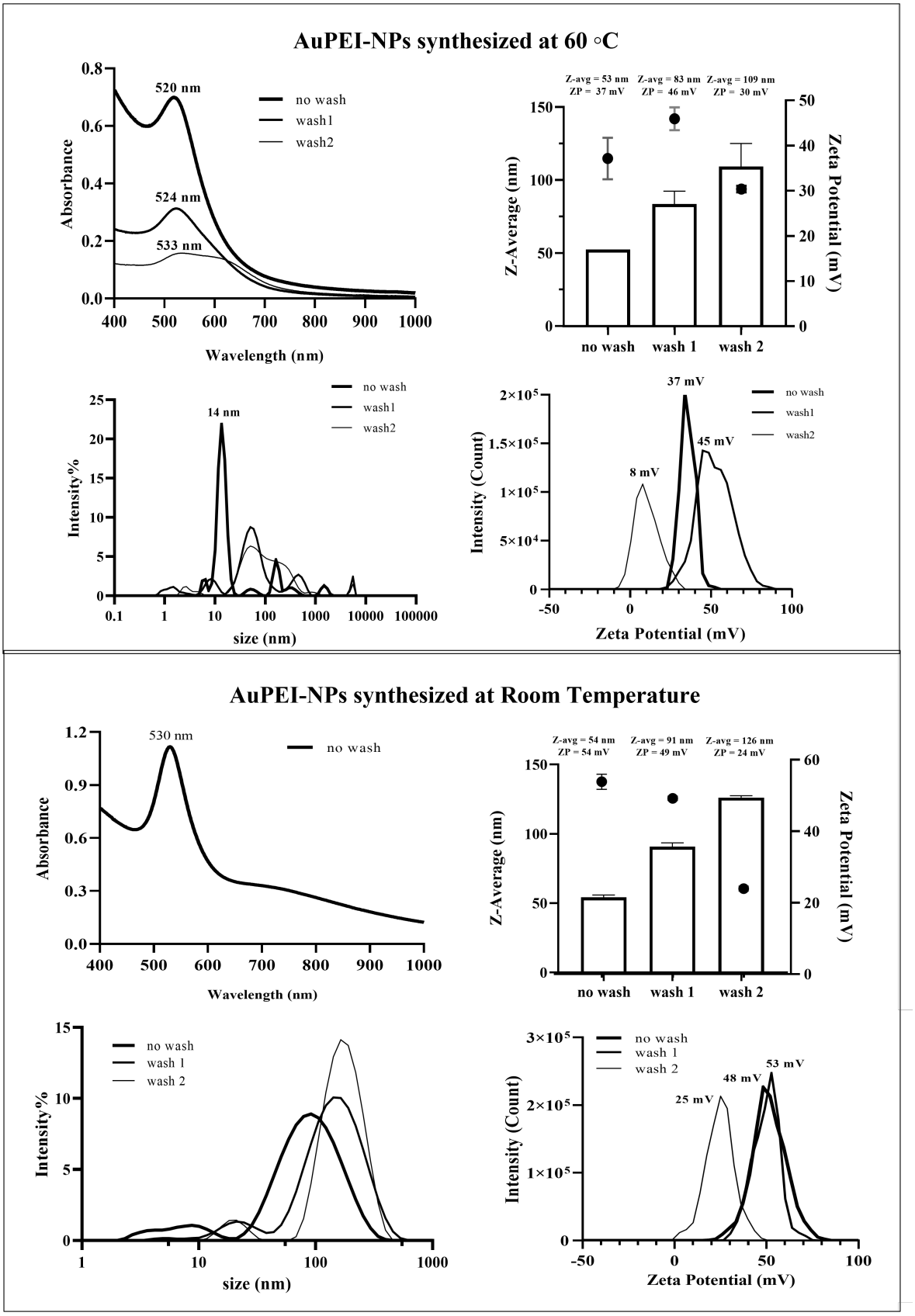

Figure 3.3 Characterisation of AuPEI-NPs synthesized at 60 °C and room temperature by Ultraviolet–visible spectroscopy and DLS after purification by centrifugation

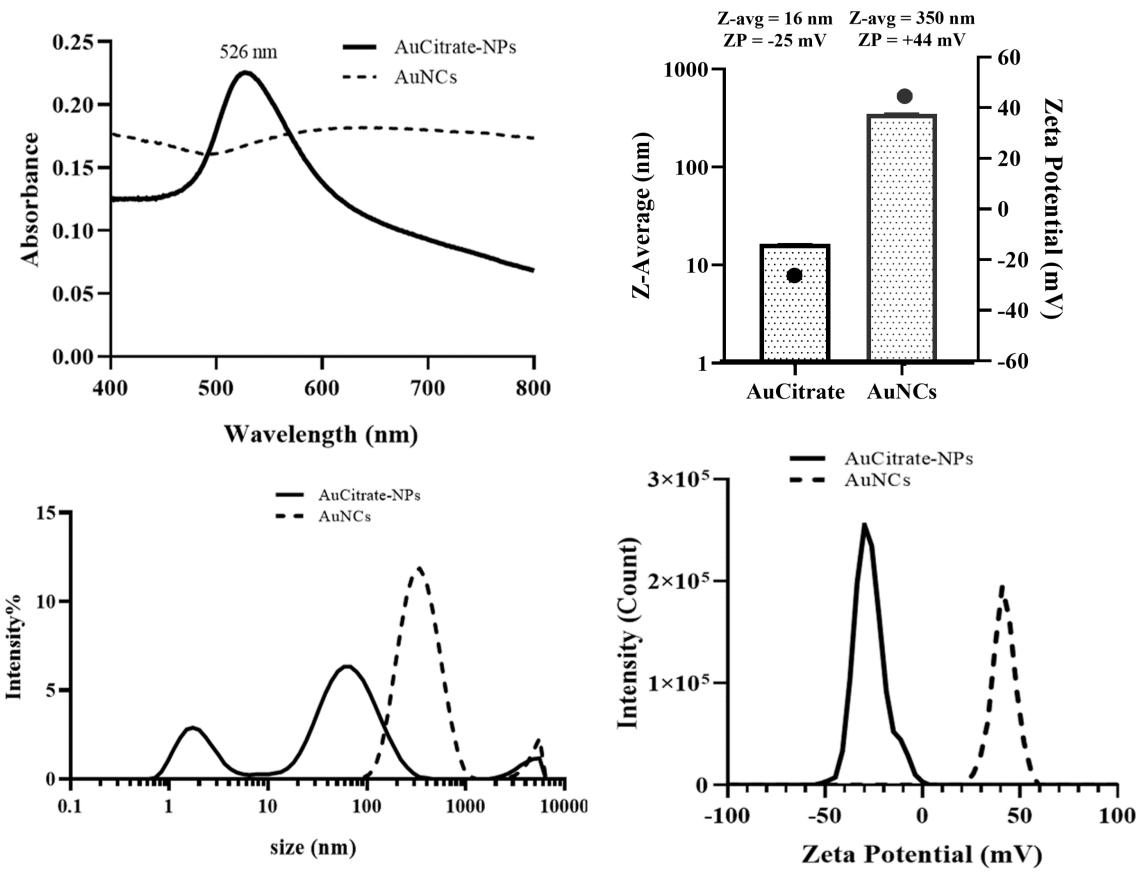

Figure 3.4 Characterisation of citrate-reduced gold nanoparticles and gold nanocones

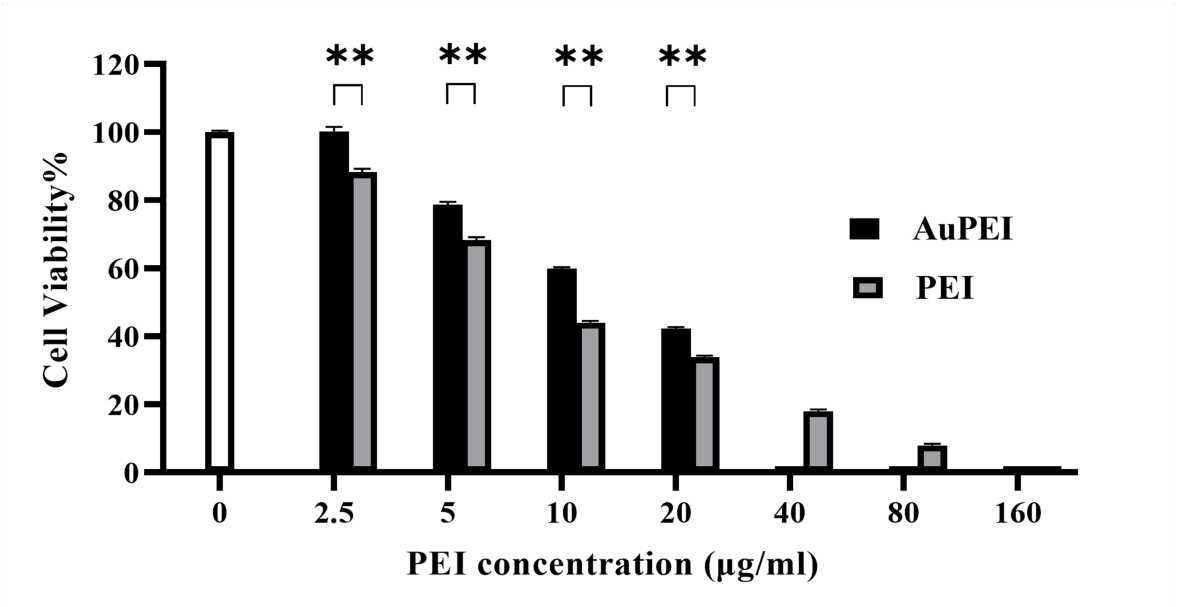

Figure 3.5 Cytotoxicity of AuPEI-NPs and free PEI on Breast Cancer Cells ($p < 0.005$). Figure was drawn with Graphpad Prism 9 Software.

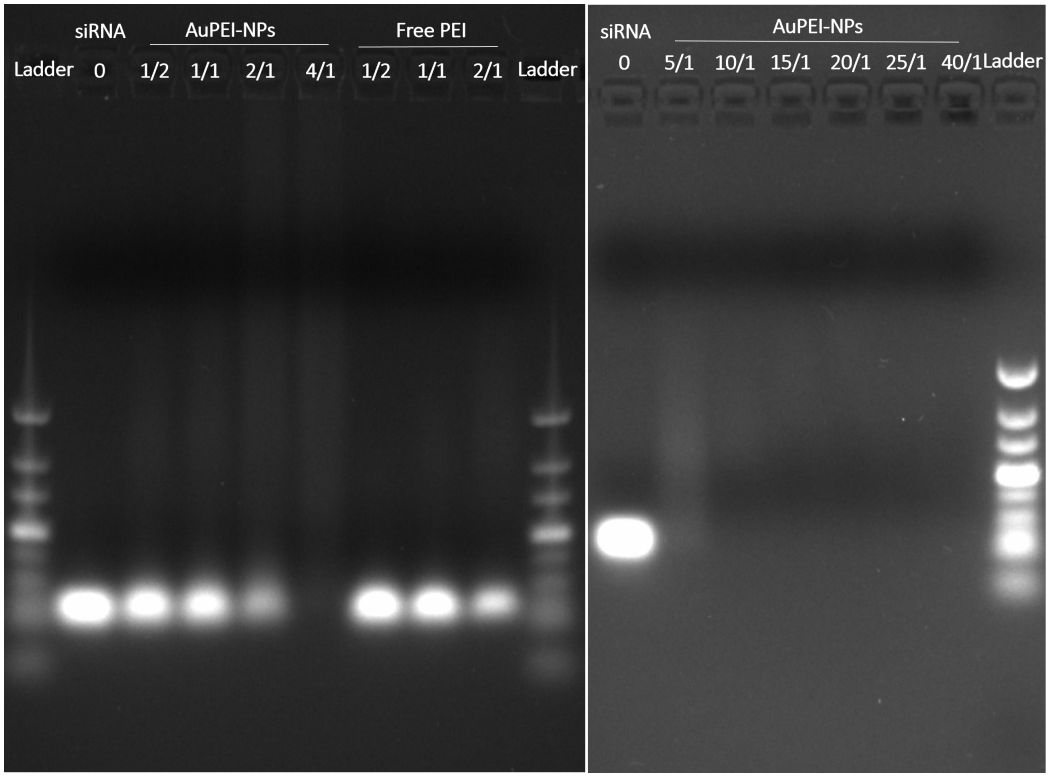

Figure 3.6 Agarose gel retardation assay demonstrated no electromotility of siRNAs at 4/1 and higher N/P ratios.

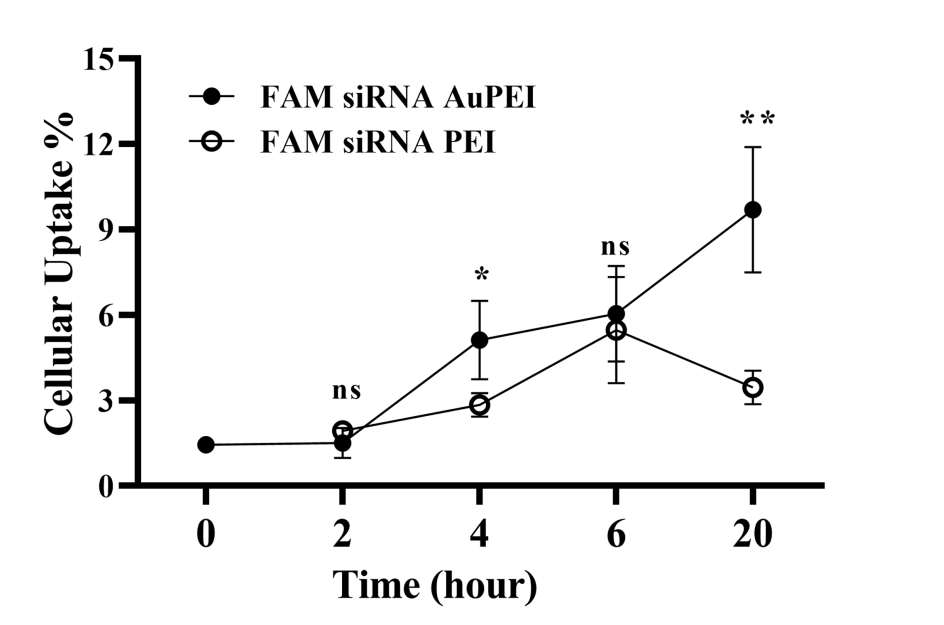

Figure 3.7 Cellular uptake of FAM-tagged siRNAs (50 nM) carried with free PEI and AuPEI-NPs into breast cancer cells (60000 cells/well) investigated by flow cytometry after 2h, 4h, 6h, and 20h (*$p<0.05$, **$p<0.005$).

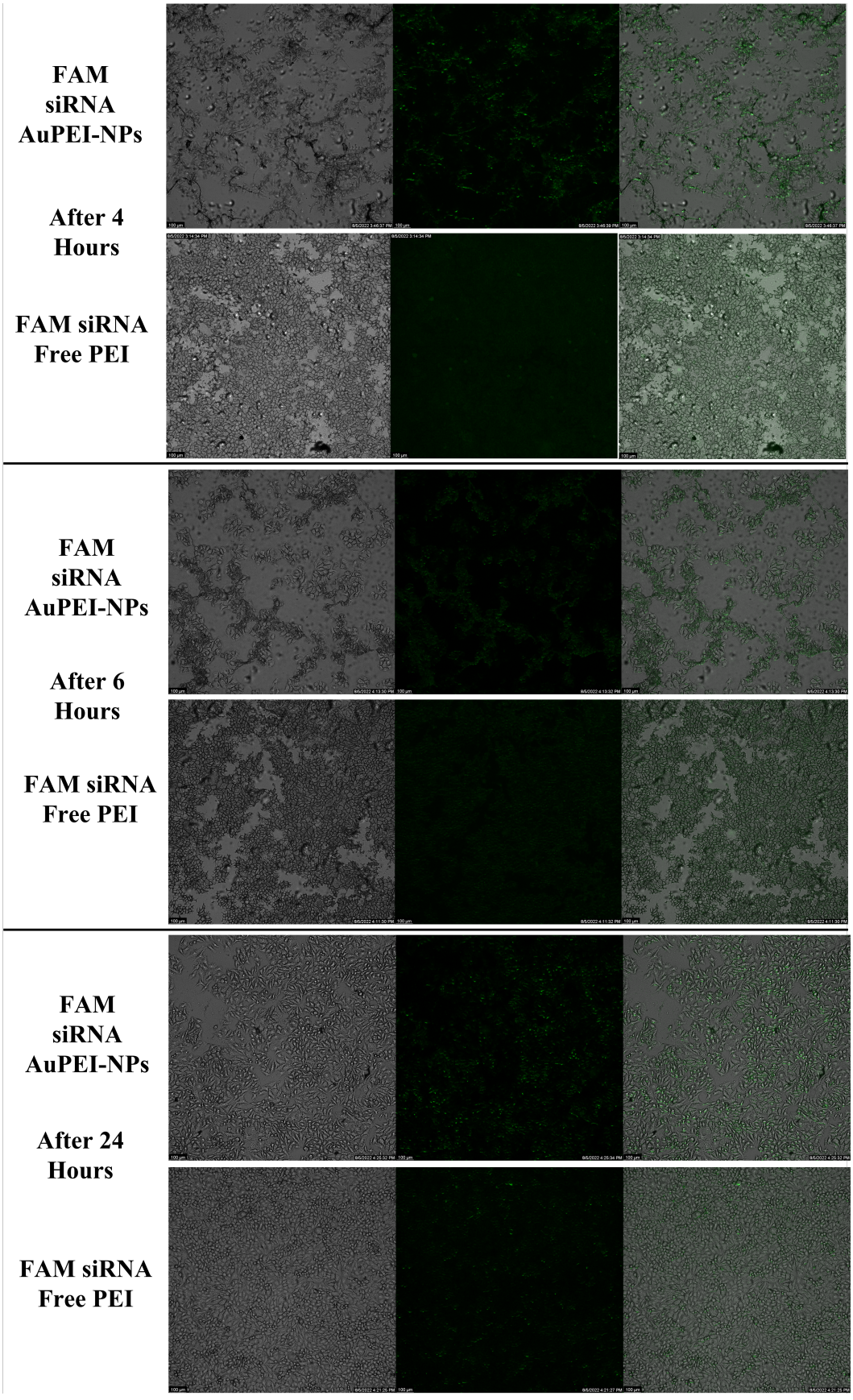

Figure 3.8 Breast cancer cells displayed by fluorescence microscopy 4, 6, and 24 hours after FAM-tagged siRNA application by free PEI and AuPEI-NPs

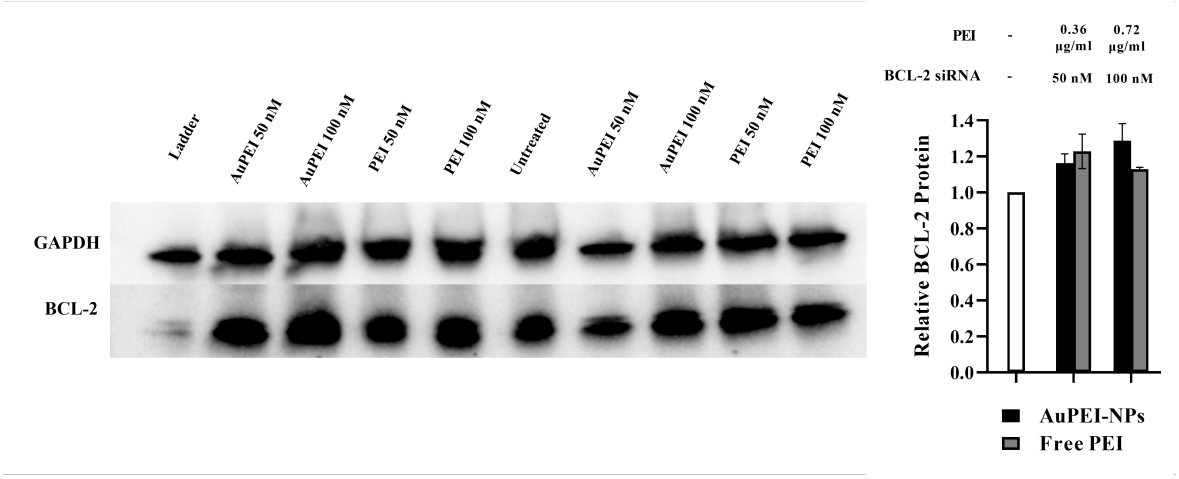

Figure 3.9 (left) Bcl-2 protein level analyzed by western blot, (right) relative Bcl-2 protein levels considering GAPDH housekeeping protein expression.

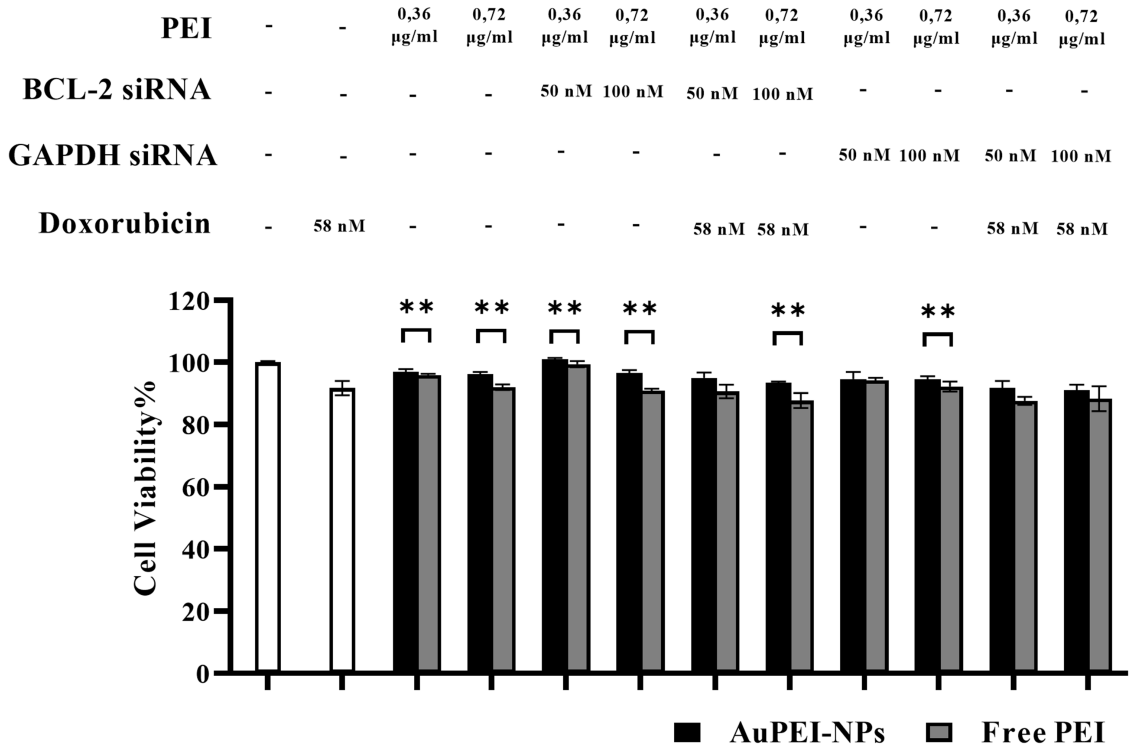

Figure 3.10 Growth inhibition of breast cancer cells (2000 cells/well) were detected by Resazurin Assay after treatment of 50 nM and 100 nM Bcl-2 siRNA carried by AuPEI-NPs and PEI.

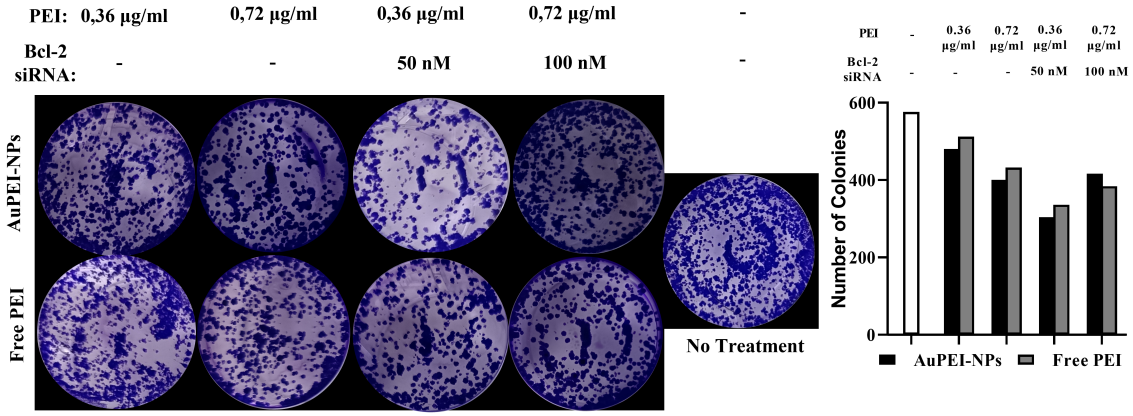

Figure 3.11 Breast cancer cell colonies were stained with crystal violet 8 days after the treatment of 50 nM and 100 nM Bcl-2 siRNA carried by AuPEI-NPs and PEI.

4. DISCUSSION

RNA interference is a powerful gene editing tool applicable in cancer therapy based on silencing oncogenic expression levels. Small interfering RNAs (siRNA) are RNAi agents that can be used to silence targeted genes with a sequence-specificity. siRNA delivery into the cells is challenging because siRNA is open to nuclease-mediated degradation inside body, negatively charged siRNA molecules are not good at passing through cellular membrane, and the delivered siRNA is a subject to endosomal entrapment. In order to achieve a successful siRNA delivery, it is a common strategy to take advantage of positively charged carrier molecules that electrostatically interact with nucleic acids [20].

Polyethylenimine (PEI) is a positively charged polymer molecule widely used in nucleic acid delivery. Thanks to the proton sponge effect caused by secondary and tertiary amine groups of PEI, an increased endosomal escape is achieved [49]. However, PEI is known to be highly toxic due to excessive positive charges. Beside electrical charge, the molecular size of PEI also contributes its cytotoxicity. Although PEI in low molecular weight has been reported nontoxic, its transfection efficiency is also restricted. Nevertheless, it has been shown that the toxicity of high molecular weight PEI could be compensated by reducing its molecular size into a compact structure, while maintaining transfection efficiency [30]. One approach to reduce the PEI molecular size is the synthesis of compact metal nanoparticle clusters with PEI [32].

Gold nanoparticles are attractive inorganic carriers due to biocompatibility, low toxicity, easy synthesis, and adaptability of surface chemistry [34]. Different gold geometries have been formulated and utilized in biomedical applications, such as gold nanospheres, nanorods, and nanostars [35].

PEI has been utilized in synthesizing positively charged gold nanoparticles for the purpose of nucleic acid delivery. In a 2010 study, polyethylenimine capped gold

nanoparticles (AuPEI-NPs) was synthesized by reduction of gold with PEI in the room temperature and conjugated with green fluorescent protein (GFP) siRNAs based on electrostatical interactions [44]. The delivery of GFP siRNAs was reported to be more effective in silencing gene expression with AuPEI-NPs than free PEI although the cellular uptake was less than in comparison to free PEI [44]. In another study, AuPEI-NPs were utilized in glutathione sensing and nucleic acid delivery [32]. Relatively easier synthesis of AuPEI-NPs was demonstrated in organic solvents such as acetyl acetone and formaldehyde and also in water at 60 °C [32].

In this project, it was aimed to synthesize polyethylenimine-capped gold nanoparticles (AuPEI-NPs) as positively charged stable nanoparticles with proper polydispersity to investigate their cytotoxicity and nucleic acid delivery in breast cancer cells in comparison to free PEI. It was also aimed to investigate the success of AuPEI-NPs in gene therapy as a carrier in delivering siRNA to silence oncogenic Bcl-2 protein expression in breast cancer cells in order to reduce cancer cell growth and colony formation.

In this research, the synthesis and characterisation of AuPEI-NPs were conducted at the room temperature, 60 °C, and 65 °C. The optimal procedure for synthesizing polyethylenimine-capped gold nanoparticles (AuPEI-NPs) were determined as reducing hydrogen tetrachloroaurate ($HAuCl_4$) at 60 °C in the presence of 25 kDa branched polyethylenimine for 15 minutes [32], which was indicated by color change from light brown to wine red, characterizing gold nanoparticle formation (Figure 3.1).

To identify the structural character of the nanoparticles, UV-vis spectroscopy was used (Figure 3.2). UV-vis spectroscopy resulted in a wavelength-absorbance plot with a maximum optical density at 520 nm, because of the gold nanoparticle surface plasmon resonance, confirming AuPEI-NP formation [44]. At the peak point, the absorbance was measured 0.7, indicating a sufficient nanoparticle concentration for the measurement.

As a further characterization, the nanoparticles were analyzed with dynamic light scattering (DLS) (Figure 3.2). DLS measured that the hydrodynamic size of the

nanoparticle was 55 nm. The polydispersity index (PDI) of the measurement was 0.210, indicating a fair polydispersity. In the size distribution plot, most of the nanoparticles were determined to have 13 nm size with 22 % intensity. The other peak size values were 6, 164, 1480 nm, which were below 5 % intensity. Dynamic light scattering demonstrated a normal distribution of zeta potential values with a peak at +37 mV, indicating positively charged stable nanoparticles.

In this study, optical density of free PEI was also determined by UV-vis spectroscopy between 400 nm and 1000 nm wavelength range (Figure 3.2). Absorbance values of PEI were smaller than 0.025 between the wavelength range. The PEI absorbance was too low to comment on the absorption character of PEI, as free PEI has no surface plasmon resonance effect [25]. Dynamic light scattering demonstrated high polydispersity of sizes with a Z-average value of 145 nm (Figure 3.2). This result might be because the polymeric structure of branched 25 kDa polyethylenimine does not constitute a compact nanoparticle. Zeta potential of PEI was measured around +5 mV, which confirms PEI as a positively charged molecule.

Purification of AuPEI-NPs from residual PEI was intended with centrifuge at 15000 rpm for 20 min. Centrifuge was applied 2 times consecutively and size and zeta potential values were characterised by UV–vis spectroscopy and DLS. The absorbance peak of the nanoparticles moved from 520 nm to 524 nm and 533 nm after centrifugation steps while the Z-average sizes moved from 53 nm to 83 nm and 109 nm (Figure 3.3). The zeta potential value of the nanoparticles did also first increase from 37 mV to 46 mV after the first centrifugation, then reduced to 30 mV after the second centrifugation step. The increase in Z-average values after centrifugation suggested some accumulation of the nanoparticles, supported by the deviation of the absorbance peak point. In the next experiments, AuPEI-NPs were utilized without purification to avoid further aggregation.

To measure the amount of PEI in AuPEI-NPs after purification by centrifuging, the need for a PEI quantification protocol arose as copper (II) sulfate was not available at the moment in the laboratory. Coomassie brilliant blue is a chemical compound used

in the Bradford assay to determine protein concentration by measuring absorbance at 595 nm in comparison to protein standard with known concentration [50]. Coomassie blue stains proteins based on electrostatic interaction between the negatively charged sulfate groups of coomassie blue and the positively charged amine groups of proteins [51].

Based on the hypothesis that coomassie blue could electrostatically interact with PEI through amine groups, the relation between PEI concentration and the absorption at 595 nm after coomassie blue staining was investigated to create a new protocol to measure the concentration of PEI inside AuPEI-NPs after purification by centrifuging. In the result, a linear relationship between absorbance at 595 nm and PEI concentration within 2 to 16 µg/ml range was obtained with an R-square of 0,97 (Figure A.1). In order to verify the PEI quantification results with coomassie blue staining, another PEI quantification protocol such as copper sulfate method should be applied.

In the experiments, AuPEI-NPs were utilized without purification step and the concentration of PEI in AuPEI-NPs was calculated based on the initial amount of PEI added in the synthesis of AuPEI-NP.

Following the production and characterization of the polyethylenimine-capped gold nanoparticles (AuPEI-NPs), their cytotoxicity to breast cancer cells was measured in various concentrations compared to free polyethylenimine (PEI) (Figure 3.5). AuPEI-NPs showed no cytotoxicity in 2.5 µg/ml concentration with 100 % cell viability, suggesting total safe use until this concentration.

On the other hand, free PEI treatment reduced breast cancer cell viability to 88 % in 2.5 µg/ml concentration, which might suggest an effect on the next cell viability experiments with the use of free PEI. It was observed that AuPEI-NPs were significantly less toxic than free PEI in 5, 10, and 20 µg/ml PEI concentrations.

Although the structure of AuPEI-NPs was not visualized with electron microscopy before cell viability experiments, it can be suggested that the positive charges

of AuPEI-NPs are probably still exposed to the outside, considering quite highly positive zeta potential of AuPEI-NPs. On the other hand, the reduced cytotoxicity of AuPEI-NPs might be attributed to building a compact and stable nanoparticle in reduced size with gold atoms in the core.

In spite of the gradual decrease in cell viability following the gradual increase in free PEI concentration, cell viability reduced abruptly to zero with the application of AuPEI-NPs in 40, 80, and 160 µg/ml concentrations, suggesting that the gold at the core of the nanoparticle has some toxicity in higher concentrations than 20 µg/ml.

Nanoparticle siRNA complexes can be characterized by measuring hydrodynamic size and zeta potential in DLS, expecting a higher size and more negative zeta potential. However, the AuPEI-NPs siRNA complexes could not be characterized by DLS because the volume of the sample was not sufficient for the analysis during the experiment. Instead, the formation of a complex between AuPEI-NPs and siRNA was demonstrated with a gel retardation assay.

Agarose gel retardation assay was conducted to determine the optimum ratio of amine to phosphate (N/P) for the siRNA nanoparticle complexes [52] (Figure 3.6). Free PEI and AuPEI-NPs were conjugated with siRNA in concentrations based on the calculations of N/P.

N/P values were calculated considering how many amine and phosphate groups each PEI and siRNA molecule are carrying. The number of monomers in a 25 kDa branched PEI molecule was determined as 582, based on molecular weights of ethylenimine monomer and polyethylenimine polymer, which are 43 g/mol and 25000 g/mol, respectively. As each ethylenimine monomer carries one amine group, it was calculated that one PEI molecule carries 582 amine groups. Considering siRNA is 21 base-pair long, one molecule of double-stranded siRNA was determined to carry 42 phosphate groups. Agarose gel retardation assay demonstrated that an N/P of 4/1 demonstrated no siRNA electromotility, concluding optimal N/P ratio as 4/1.

Cellular internalization of FAM-tagged siRNAs by AuPEI-NPs and free PEI to breast cancer cells was investigated with flow cytometry aiming to observe FAM-tagged siRNAs (Figure 3.7). After the 2nd hour of the treatment, no cellular internalization was observed. 4 hour following the treatment, 5.1 % of the cells were determined with AuPEI-NPs uptake, significantly more than free PEI with 2.8 % of nanoparticle uptake. After the 6th hour of the treatment, the cellular uptake with free PEI as 5.5 % was not significantly less than AuPEI-NPs as 6.0 %, suggesting that cellular uptake of PEI was happening at a slower rate than AuPEI-NPs. Increased cellular uptake of AuPEI-NPs could be because of their solid molecular structure compared to the messy molecular structure of branched polyethylenimine. After the 20th hour of the treatment, the cellular uptake of AuPEI-NPs increased to 9.7 %, while the uptake of free PEI reduced to 3.4 %, suggesting that free PEI might be prone to endosomal entrapment and exocytosis more than AuPEI-NPs.

After flow cytometry, the cellular internalization of FAM-tagged siRNAs into breast cancer cells was also investigated under a fluorescence microscope (Figure 3.8). Fluorescence microscopy confirmed the delivery of FAM-tagged siRNAs into breast cancer cells with AuPEI-NPs after 4th, 6th, and 24th hours of the treatment. Cellular uptake was observed better with AuPEI-NPs than free PEI after 4th, 6th and 24th hours of the treatment. Cellular uptake with free PEI was very low at 4th and 6th hours of the treatment and better uptake was observed at the 24th hour of the treatment. The results concluded that siRNA delivery took place with AuPEI-NPs better than free PEI.

To investigate the efficiency of gene silencing with Bcl-2 siRNAs delivered by AuPEI-NPs and free PEI, Bcl-2 protein levels of breast cancer cells were determined by western blot. This demonstrated no Bcl-2 reduction in breast cancer cells with Bcl-2 siRNA carried with AuPEI-NPs and free PEI (Figure 3.9).

The situation where Bcl-2 siRNA was not effective in reducing Bcl-2 protein expression level of breast cancer cells might be because the siRNA stock used in the experiment was not intact during the experimental procedure. The inability to reduce

Bcl-2 protein level would make the therapeutic effect of Bcl-2 siRNA delivery questionable in the next experiments. To validate the expression results from the western blot experiment, qRT-PCR analysis can be can be conducted to determine Bcl-2 gene expression in the mRNA level. In order to investigate gene silencing effect of the siRNA delivery with AuPEI-NPs and free PEI, the expression level of GAPDH protein might be investigated with western blot and GAPDH activity assay following the delivery of GAPDH siRNAs by AuPEI-NPs and PEI.

Growth inhibition of breast cancer cells were studied by resazurin assay after treatments with 50 nM and 100 nM of Bcl-2 siRNAs and GAPDH siRNAs carried by AuPEI-NPs and free PEI combined with doxorubicin IC 20 (Figure 3.10). Treatment with doxorubicin IC 20 resulted in 91.7 % of cell viability. As IC 20 value theoretically predicts a cell viability of 80 %, the high cell viability with IC 20 doxorubicin treatment might suggest that the incubation time of the cells, which was 72 hours, was long enough for the recovery and reproduction of the breast cancer cells. IC 20 values were calculated based on a previous study with the same MDA-MB-231 cell lineage [53]. The generation of breast cancer cells in the experiment might have developed further resistance to DOX, contributing their increased viability.

In part due to less cytotoxicity of AuPEI-NPs compared to free PEI, delivery with AuPEI-NPs resulted in more cellular viability than free PEI in all experimental groups (Figure 3.10). Free PEI induced growth inhibition significantly more than AuPEI-NPs, which was noncontradictory to the cytotoxicity experiment in Figure 3.5. Treatment with 100 nM Bcl-2 siRNA carried by free PEI reduced cellular viability to 90.9 %, suggesting significantly more growth inhibition than the delivery with AuPEI-NPs (Figure 3.10). Although this cell viability was less than that of DOX IC 20, the difference was not statistically significant. The statisticaly insignificant results for doxorubicin IC 20 and Bcl-2 and GAPDH siRNAs might be because of relatively smaller sample size.

Combined therapy of doxorubicin IC 20 and 100 nM Bcl-2 siRNA carried by free PEI reduced cellular viability to 87.7 %, suggesting more growth inhibition than DOX

IC 20 alone (Figure 3.10). Even though the difference was statistically insignificant with a p value of 0.055, repetition of the experiment with a larger sample size might reveal a more evidential result.

The treatment with 50 nM of GAPDH siRNAs carried by both AuPEI-NPs and free PEI and 100 nM of siRNAs by AuPEI-NPs reduced cell viability to 94 %, suggesting statistically more growth inhibition than their Bcl-2 counterparts. The treatment with 100 nM GAPDH siRNA carried by PEI reduced cellular viability to 92.2 %, suggesting significantly more growth inhibition than the delivery with AuPEI-NPs (Figure 3.10).

Combined therapy of DOX IC 20 and GAPDH siRNA carried by free PEI reduced cellular viability to 87.6 % for 50 nM and 88.3 % for 100 nM siRNA concentrations (Figure 3.10). In general, the treatment with Bcl-2 siRNAs was not statistically more successful than GAPDH siRNAs in reducing growth inhibition of breast cancer cells. The inefficacy in the inhibition with Bcl-2 siRNA delivery by AuPEI-NPs and free PEI might be because of the inability of Bcl-2 silencing after Bcl-2 siRNA delivery observed by western blot experiment (Figure 3.9).

Colony formation assay with crystal violet was applied to investigate the effect of Bcl-2 siRNA carried by free PEI and AuPEI-NPs on breast cancer cells. Untreated breast cancer cells formed slightly denser colonies than the treatment groups. 50 nM Bcl-2 siRNA carried by AuPEI-NPs decreased the number of colonies the most (Figure 3.11). Considering that Bcl-2 siRNA carried by PEI induced more growth inhibition than AuPEI-NPs in the growth inhibition assay, it can be concluded that Bcl-2 siRNA carried by AuPEI-NPs reduced colony formation more than free PEI. In the experiment, the high density of colonies on the plate suggested that the number of cells was higher than sufficient which was 1000 cells in 250 µl medium per well. The incubation time for colony formation as 8 days could have also affected the excessive number of colonies.

In this thesis, the synthesis of polyethylenimine-capped gold nanoparticles (AuPEI-NPs) were conducted relatively easily and effectively at 60 °C in comparison to room temperature and 65 °C. AuPEI-NPs were demonstrated to be considerably safe until

2.5 µg/ml concentration and less toxic in comparison to free PEI to breast cancer cells. Cellular uptake of AuPEI-NPs was also higher than free PEI. In conclusion, AuPEI-NPs are promising in nucleic acid delivery applications as easily synthesized, safe, and positively charged carriers.

For the future, some complementary experiments to this study can be planned. In order to achieve a further characterisation of AuPEI-NPs, electron microscopy images of the nanoparticles can be obtained. Nanoparticle Tracking Analysis (NTA) of AuPEI-NPs can be applied to measure the number and size of the nanoparticles. Characterisation of AuPEI-NPs siRNA complexes can also be conducted with UV-vis spectroscopy and DLS.

In the future, the repeat of Bcl-2 siRNA delivery to breast cancer cells could be can to verify previous results. Western blot experiment should be applied with a positive control group with effective Bcl-2 silencing in order to conclude the efficiency or inefficiency of the treatment. Moreover, the repeat of growth inhibition and colony formation experiments can be conducted with reduced number of initial cells and shorter incubation period to avoid excessive cellular growth and colony formation.

As a future perspective, the efficiency of AuPEI-NPs in nucleic acid delivery could be explored further with various gene targets in combined therapeutic applications in comparison to other nucleic acid delivery systems. As a further stage of the gene delivery application, the *in vivo* potential of AuPEI-NPs could be investigated following affirmative *in vitro* gene therapy results in various cancer cell lines.

REFERENCES

1. Arnold, M., E. Morgan, H. Rumgay, A. Mafra, D. Singh, M. Laversanne, J. Vignat, J. R. Gralow, F. Cardoso, S. Siesling *et al.*, "Current and future burden of breast cancer: Global statistics for 2020 and 2040", *The Breast*, Vol. 66, pp. 15–23, 2022.

2. Li, C., Y. Wang, H. Zhang, M. Li, Z. Zhu and Y. Xue, "An investigation on the cytotoxicity and caspase-mediated apoptotic effect of biologically synthesized gold nanoparticles using Cardiospermum halicacabum on AGS gastric carcinoma cells", *International journal of nanomedicine*, Vol. 14, p. 951, 2019.

3. Mohamed, A. N., "BCL2 (B-Cell Leukemia/Lymphoma 2)", , 2018.

4. Carvalho, C., R. X. Santos, S. Cardoso, S. Correia, P. J. Oliveira, M. S. Santos and P. I. Moreira, "Doxorubicin: the good, the bad and the ugly effect", *Current medicinal chemistry*, Vol. 16, No. 25, pp. 3267–3285, 2009.

5. Qin, S.-Y., Y.-J. Cheng, Q. Lei, A.-Q. Zhang and X.-Z. Zhang, "Combinational strategy for high-performance cancer chemotherapy", *Biomaterials*, Vol. 171, pp. 178–197, 2018.

6. Duarte, D. and N. Vale, "Evaluation of synergism in drug combinations and reference models for future orientations in oncology", *Current Research in Pharmacology and Drug Discovery*, p. 100110, 2022.

7. Unniyampurath, U., R. Pilankatta and M. N. Krishnan, "RNA interference in the age of CRISPR: will CRISPR interfere with RNAi?", *International journal of molecular sciences*, Vol. 17, No. 3, p. 291, 2016.

8. Obbard, D. J., K. H. Gordon, A. H. Buck and F. M. Jiggins, "The evolution of RNAi as a defence against viruses and transposable elements", *Philosophical Transactions of the Royal Society B: Biological Sciences*, Vol. 364, No. 1513, pp. 99–115, 2009.

9. Silva, R., D. Ferreira and L. R. Rodrigues, "Exosome-based delivery of RNAi leads to breast cancer inhibition", *Journal of Drug Delivery Science and Technology*, Vol. 78, p. 103931, 2022.

10. Koo, K. M., L. G. Carrascosa, M. J. Shiddiky and M. Trau, "Poly (A) extensions of miRNAs for amplification-free electrochemical detection on screen-printed gold electrodes", *Analytical chemistry*, Vol. 88, No. 4, pp. 2000–2005, 2016.

11. Cambronne, X. A., R. Shen, P. L. Auer and R. H. Goodman, "Capturing microRNA targets using an RNA-induced silencing complex (RISC)-trap approach", *Proceedings of the National Academy of Sciences*, Vol. 109, No. 50, pp. 20473–20478, 2012.

12. Halbur, C., N. Choudhury, M. Chen, J. H. Kim and E. J. Chung, "siRNA-conjugated nanoparticles to treat ovarian cancer", *SLAS TECHNOLOGY: Translating Life Sciences Innovation*, Vol. 24, No. 2, pp. 137–150, 2019.

13. Alvandifar, F., B. Ghaffari, N. Goodarzi, N. S. Ravari, F. Karami, M. Amini, E. Souri, M. R. Khoshayand, M. Esfandyari-Manesh, R. M. Jafari *et al.*, "Dual drug delivery system of PLGA nanoparticles to reverse drug resistance by altering BAX/Bcl-2", *Journal of Drug Delivery Science and Technology*, Vol. 47, pp. 291–298, 2018.

14. Inao, T., Y. Iida, T. Moritani, T. Okimoto, R. Tanino, H. Kotani and M. Harada, "Bcl-2 inhibition sensitizes triple-negative human breast cancer cells to doxorubicin", *Oncotarget*, Vol. 9, No. 39, p. 25545, 2018.

15. Sun, W., X.-Y. Liu, L.-L. Ma and Z.-L. Lu, "Tumor targeting gene vector for visual tracking of Bcl-2 siRNA transfection and anti-tumor therapy", *ACS applied materials & interfaces*, Vol. 12, No. 9, pp. 10193–10201, 2020.

16. Vocelle, D., C. Chan and S. P. Walton, "Endocytosis controls siRNA efficiency: implications for siRNA delivery vehicle design and cell-specific targeting", *nucleic acid therapeutics*, Vol. 30, No. 1, pp. 22–32, 2020.

17. Hu, B., L. Zhong, Y. Weng, L. Peng, Y. Huang, Y. Zhao and X.-J. Liang, "Therapeutic siRNA: state of the art", *Signal transduction and targeted therapy*, Vol. 5, No. 1, p. 101, 2020.

18. Kulkarni, J. A., D. Witzigmann, S. B. Thomson, S. Chen, B. R. Leavitt, P. R. Cullis and R. van der Meel, "The current landscape of nucleic acid therapeutics", *Nature nanotechnology*, Vol. 16, No. 6, pp. 630–643, 2021.

19. Du Rietz, H., H. Hedlund, S. Wilhelmson, P. Nordenfelt and A. Wittrup, "Imaging small molecule-induced endosomal escape of siRNA", *Nature communications*, Vol. 11, No. 1, p. 1809, 2020.

20. Choi, Y. S., M. Y. Lee, A. E. David and Y. S. Park, "Nanoparticles for gene delivery: therapeutic and toxic effects", *Molecular & cellular toxicology*, Vol. 10, pp. 1–8, 2014.

21. Yang, Y., Z. Liu, H. Ma and M. Cao, "Application of Peptides in Construction of Nonviral Vectors for Gene Delivery", *Nanomaterials*, Vol. 12, No. 22, p. 4076, 2022.

22. Dreaden, E. C., L. A. Austin, M. A. Mackey and M. A. El-Sayed, "Size matters: gold nanoparticles in targeted cancer drug delivery", *Therapeutic delivery*, Vol. 3, No. 4, pp. 457–478, 2012.

23. Wilson, B. and K. M. Geetha, "Lipid nanoparticles in the development of mRNA vaccines for COVID-19", *Journal of Drug Delivery Science and Technology*, Vol. 74, p. 103553, 2022.

24. Lungu, C. N., M. V. Diudea, M. V. Putz and I. P. Grudziński, "Linear and branched PEIs (polyethylenimines) and their property space", *International Journal of Molecular Sciences*, Vol. 17, No. 4, p. 555, 2016.

25. Ungaro, F., G. De Rosa, A. Miro and F. Quaglia, "Spectrophotometric determination of polyethylenimine in the presence of an oligonucleotide for the characterization of controlled release formulations", *Journal of pharmaceutical and biomedical analysis*, Vol. 31, No. 1, pp. 143–149, 2003.

26. Benjaminsen, R. V., M. A. Mattebjerg, J. R. Henriksen, S. M. Moghimi and T. L. Andresen, "The possible "proton sponge" effect of polyethylenimine (PEI) does not include change in lysosomal pH", *Molecular Therapy*, Vol. 21, No. 1, pp. 149–157, 2013.

27. El-Sayed, A., S. Futaki and H. Harashima, "Delivery of macromolecules using arginine-rich cell-penetrating peptides: ways to overcome endosomal entrapment", *The AAPS journal*, Vol. 11, pp. 13–22, 2009.

28. Kafil, V. and Y. Omidi, "Cytotoxic impacts of linear and branched polyethylenimine nanostructures in a431 cells", *BioImpacts: BI*, Vol. 1, No. 1, p. 23, 2011.

29. Fischer, D., T. Bieber, Y. Li, H.-P. Elsässer and T. Kissel, "A novel non-viral vector for DNA delivery based on low molecular weight, branched polyethylenimine: effect of molecular weight on transfection efficiency and cytotoxicity", *Pharmaceutical research*, Vol. 16, pp. 1273–1279, 1999.

30. Neu, M., D. Fischer and T. Kissel, "Recent advances in rational gene transfer vector design based on poly (ethylene imine) and its derivatives", *The Journal of Gene Medicine: A cross-disciplinary journal for research on the science of gene transfer and its clinical applications*, Vol. 7, No. 8, pp. 992–1009, 2005.

31. Forrest, M. L., J. T. Koerber and D. W. Pack, "A degradable polyethylenimine derivative with low toxicity for highly efficient gene delivery", *Bioconjugate chemistry*, Vol. 14, No. 5, pp. 934–940, 2003.

32. Pandey, P. C., G. Pandey and R. J. Narayan, "Controlled synthesis of polyethylenimine coated gold nanoparticles: Application in glutathione sensing and nucleotide delivery", *Journal of Biomedical Materials Research Part B: Applied Biomaterials*, Vol. 105, No. 5, pp. 1191–1199, 2017.

33. Paul, W. and C. P. Sharma, "Inorganic nanoparticles for targeted drug delivery", *Biointegration of medical implant materials*, pp. 333–373, 2020.

34. Silva, T. R. and I. C. Vieira, "A biosensor based on gold nanoparticles stabilized in poly (allylamine hydrochloride) and decorated with laccase for determination of dopamine", *Analyst*, Vol. 141, No. 1, pp. 216–224, 2016.

35. Yue, J., T. J. Feliciano, W. Li, A. Lee and T. W. Odom, "Gold nanoparticle size and shape effects on cellular uptake and intracellular distribution of siRNA nanoconstructs", *Bioconjugate chemistry*, Vol. 28, No. 6, pp. 1791–1800, 2017.

36. Zhu, X., C. Vo, M. Taylor and B. R. Smith, "Non-spherical micro-and nanoparticles in nanomedicine", *Materials Horizons*, Vol. 6, No. 6, pp. 1094–1121, 2019.

37. Makvandi, P., A. Zarepour, X. Zheng, T. Agarwal, M. Ghomi, R. Sartorius, E. N. Zare, A. Zarrabi, A. Wu, T. K. Maiti *et al.*, "Non-spherical nanostructures in nanomedicine: From noble metal nanorods to transition metal dichalcogenide nanosheets", *Applied Materials Today*, Vol. 24, p. 101107, 2021.

38. Huang, X. and M. A. El-Sayed, "Gold nanoparticles: Optical properties and implementations in cancer diagnosis and photothermal therapy", *Journal of advanced research*, Vol. 1, No. 1, pp. 13–28, 2010.

39. Rahman, S., "Size and concentration analysis of gold nanoparticles with ultraviolet-visible spectroscopy", *Undergrad J Math Model One+ Two*, Vol. 7, p. 13, 2016.

40. Dong, J., P. L. Carpinone, G. Pyrgiotakis, P. Demokritou and B. M. Moudgil, "Synthesis of precision gold nanoparticles using Turkevich method", *KONA Powder and Particle Journal*, Vol. 37, pp. 224–232, 2020.

41. Tunç, C. U., D. Y. Öztaş, D. Uzunoğlu, Ö. F. Bayrak and M. Çulha, "Silencing breast cancer genes using morpholino embedded DNA-tile-AuNPs nanostructures", *Human gene therapy*, Vol. 30, No. 12, pp. 1547–1558, 2019.

42. Kim, K., H. B. Lee, J. W. Lee, H. K. Park and K. S. Shin, "Self-assembly of poly (ethylenimine)-capped Au nanoparticles at a toluene- water interface for efficient surface-enhanced Raman scattering", *Langmuir*, Vol. 24, No. 14, pp. 7178–7183, 2008.

43. Cebrián, V., F. Martín-Saavedra, C. Yagüe, M. Arruebo, J. Santamaría and N. Vilaboa, "Size-dependent transfection efficiency of PEI-coated gold nanoparticles", *Acta Biomaterialia*, Vol. 7, No. 10, pp. 3645–3655, 2011.

44. Song, W.-J., J.-Z. Du, T.-M. Sun, P.-Z. Zhang and J. Wang, "Gold nanoparticles capped with polyethyleneimine for enhanced siRNA delivery", *small*, Vol. 6, No. 2, pp. 239–246, 2010.

45. Rahme, K., J. Guo and J. D. Holmes, "Bioconjugated gold nanoparticles enhance siRNA delivery in prostate cancer cells", *RNA Interference and Cancer Therapy: Methods and Protocols*, pp. 291–301, 2019.

46. Pong, B.-K., H. I. Elim, J.-X. Chong, W. Ji, B. L. Trout and J.-Y. Lee, "New insights on the nanoparticle growth mechanism in the citrate reduction of gold (III) salt: formation of the Au nanowire intermediate and its nonlinear optical properties", *The Journal of Physical Chemistry C*, Vol. 111, No. 17, pp. 6281–6287, 2007.

47. Kip, B., C. U. Tunc and O. Aydin, "Triple-combination therapy assisted with ultrasound-active gold nanoparticles and ultrasound therapy against 3D cisplatin-resistant ovarian cancer model", *Ultrasonics Sonochemistry*, Vol. 82, p. 105903, 2022.

48. Van Tonder, A., A. M. Joubert and A. D. Cromarty, "Limitations of the 3-(4, 5-dimethylthiazol-2-yl)-2, 5-diphenyl-2H-tetrazolium bromide (MTT) assay when compared to three commonly used cell enumeration assays", *BMC research notes*, Vol. 8, pp. 1–10, 2015.

49. Chen, Z., L. Zhang, Y. He and Y. Li, "Sandwich-type Au-PEI/DNA/PEI-Dexa nanocomplex for nucleus-targeted gene delivery in vitro and in vivo", *Acs Applied Materials & Interfaces*, Vol. 6, No. 16, pp. 14196–14206, 2014.

50. Yang, M., D. Shi, Y. Wang, A. G. Ebadi and M. Toughani, "Study on Interaction of Coomassie Brilliant Blue G-250 with Bovine Serum Albumin by Multispectroscopic", *International Journal of Peptide Research and Therapeutics*, Vol. 27, pp. 421–431, 2021.

51. Tal, M., A. Silberstein and E. Nusser, "Why does Coomassie Brilliant Blue R interact differently with different proteins? A partial answer.", *Journal of biological chemistry*, Vol. 260, No. 18, pp. 9976–9980, 1985.

52. Aydin, O., D. Kanarya, U. Yilmaz and C. Ü. Tunç, "Determination of optimum ratio of cationic polymers and small interfering RNA with agarose gel retardation assay", *Antisense RNA Design, Delivery, and Analysis*, pp. 117–128, Springer US New York, NY, 2022.

53. Walweel, N. S. M. S., *The effect of LC3 siRNA and doxorubicin dual treatment against breast cancer*, Master's Thesis, 2022.

APPENDIX A. Quantification of Polyethylenimine by Coomassie Blue Staining

Table A.1 Calculation of PEI concentration (μg/ml) by coomassie staining in the supernatant and the percentage of PEI in AuPEI-NPs after purification by centrifuge

AuPEI-NPs	**Initial PEI concentration (μg/ml)**	**PEI (μg/ml) in Supernatant 1**	**PEI % in AuPEI-NPs after centrifuge 1**	**PEI (μg/ml) in Supernatant 2**	**PEI % in AuPEI-NPs after centrifuge 2**
Synthesized at 60 °C	2140	657	69.3 %	101	64.5 %
Synthesized at RT	195	152	22 %	0	22 %

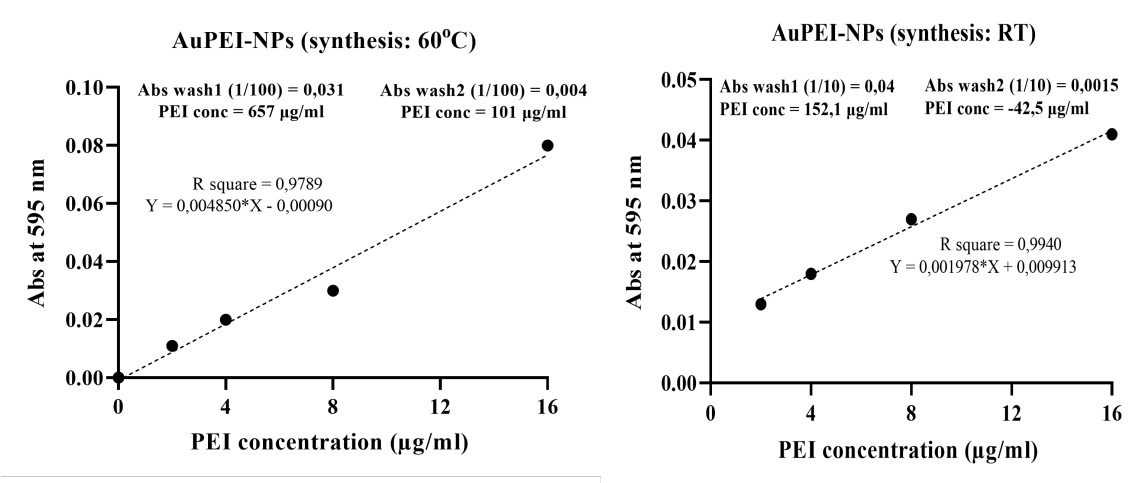

Figure A.1 Quantification of Polyethylenimine by Coomassie Blue Staining

APPENDIX B. Quantification of the Total Protein by Coomassie Blue Staining

Table B.1 Calculation of the total protein concentration (mg/ml) from the cell extracts based on absorbance at 595 nm in reference to BSA standard curve

Experiment group	**Absorbance (1/10)**	**Protein concentration (mg/ml)**
AuPEI-NPs 50 nM siRNA	0.709	5.803
AuPEI-NPs 100 nM siRNA	0.629	5.159
PEI 50 nM siRNA	0.766	6.259
PEI 100 nM siRNA	0.69	5.651
No Treatment	0.644	5.283

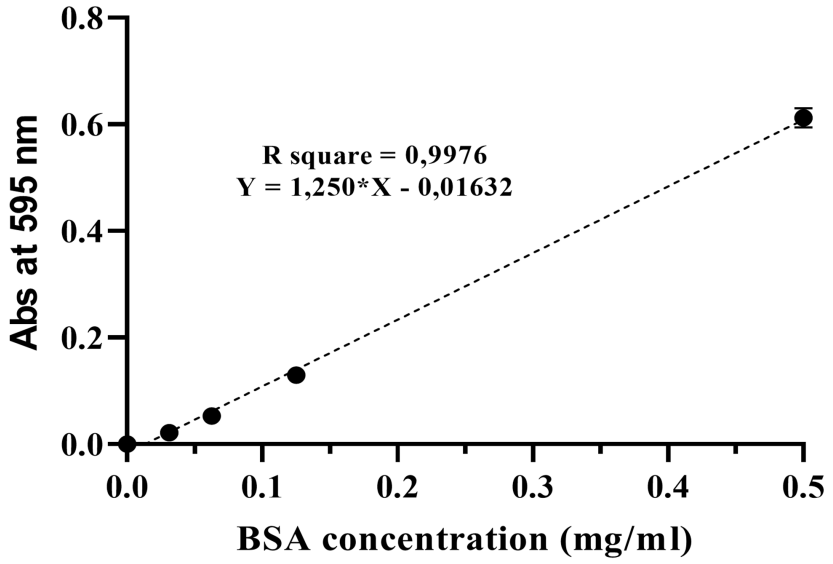

Figure B.1 Standard curve for the absorbance values of bovine serum albumin (BSA) in known concentrations after coomassie blue staining